expression of mannose-binding lectin controls athero-sclerosis in low-density lipoprotein receptor-deficient mice. *Circulation* **119**, 2188–2195

4. Fraser, D.A. and Tenner, A.J. (2010) Innate immune proteins C1q and mannan-binding lectin enhance clearance of atherogenic lipoproteins by human monocytes and macrophages. *J. Immunol.* **185**, 3932–3939

5. Naito, H., Ikeda, A., Hasegawa, K., Oka, S., Uemura, K., Kawasaki, N., and Kawasaki, T. (1999) Characterization of human serum mannan-binding protein promoter. *J. Biochem.* **126**, 1004–1012

6. Mangelsdorf, D.J., Thummel, C., Beato, M., Herrlich, P., Schutz, G., Umesono, K., Blumberg, B., Kastner, P., Mark, M., Chambon, P., and Evans, R.M. (1995) The nuclear receptor superfamily: the second decade. *Cell* **83**, 835–839

7. Fruchart, J.C. (2009) Peroxisome proliferator-activated receptor-alpha (PPARalpha): at the crossroads of obesity, diabetes and cardiovascular disease. *Atherosclerosis* **205**, 1–8

8. Tontonoz, P. and Spiegelman, B.M. (2008) Fat and beyond: the diverse biology of PPARgamma. *Annu. Rev. Biochem.* **77**, 289–312

9. Duval, C., Chinetti, G., Trottein, F., Fruchart, J.C., and Staels, B. (2002) The role of PPARs in atherosclerosis. *Trends Mol. Med* **8**, 422–430

10. Tachibana, K., Kobayashi, Y., Tanaka, T., Tagami, M., Sugiyama, A., Katayama, T., Ueda, C., Yamasaki, D., Ishimoto, K., Sumitomo, M., Uchiyama, Y., Kohro, T., Sakai, J., Hamakubo, T., Kodama, T., and Doi, T. (2005) Gene expression profiling of potential peroxisome proliferator-activated receptor (PPAR) target genes in human hepatoblastoma cell lines inducibly expressing different PPAR isoforms. *Nucl. Recept.* **3**, 3

11. Tachibana, K., Anzai, N., Ueda, C., Katayama, T., Yamasaki, D., Kirino, T., Takahashi, R., Ishimoto, K., Komori, H., Tanaka, T., Hamakubo, T., Ueda, Y., Arai, H., Sakai, J., Kodama, T., and Doi, T. (2008) Regulation of the human PDZK1 expression by peroxisome proliferator-activated receptor alpha. *FEBS Lett.* **582**, 3884–3888

12. Taylor, M.E., Brickell, P.M., Craig, R.K., and Summerfield, J.A. (1989) Structure and evolutionary origin of the gene encoding a human serum mannose-binding protein. *Biochem. J.* **262**, 763–771

13. Osumi, T., Wen, J.K., and Hashimoto, T. (1991) Two cis-acting regulatory sequences in the peroxisome proliferator-responsive enhancer region of rat acyl-CoA oxidase gene. *Biochem. Biophys. Res. Commun.* **175**, 866–871

14. Neve, B.P., Fruchart, J.C., and Staels, B. (2000) Role of the peroxisome proliferator-activated receptors (PPAR) in atherosclerosis. *Biochem. Pharmacol.* **60**, 1245–1250

15. Wada, M., Itoh, N., Ohta, M., and Kawasaki, T. (1992) Characterization of rat liver mannan-binding protein gene. *J. Biochem.* **111**, 66–73

16. Rakhshandehroo, M., Stienstra, R., de Wit, N.J., Bragt, M.C., Haluzik, M., Mensink, R.P., Muller, M., and Kersten, S. (2012) Plasma mannose-binding lectin is stimulated by PPARalpha in humans. *Am. J. Physiol. Endocrinol. Metab.* **302**, E595–E602

17. Vu-Dac, N., Chopin-Delannoy, S., Gervois, P., Bonnelye, E., Martin, G., Fruchart, J.C., Laudet, V., and Staels, B. (1998) The nuclear receptors peroxisome proliferator-activated receptor alpha and Rev-erbalpha mediate the species-specific regulation of apolipoprotein A-I expression by fibrates. *J. Biol. Chem.* **273**, 25713–25720

Long-Term Self-Renewal of Human ES/iPS-Derived Hepatoblast-like Cells on Human Laminin 111-Coated Dishes

Kazuo Takayama,[1,2,3] Yasuhito Nagamoto,[1,2] Natsumi Mimura,[2] Katsuhisa Tashiro,[4] Fuminori Sakurai,[1] Masashi Tachibana,[1] Takao Hayakawa,[5] Kenji Kawabata,[4] and Hiroyuki Mizuguchi[1,2,3,6,*]

[1]Laboratory of Biochemistry and Molecular Biology, Graduate School of Pharmaceutical Sciences, Osaka University, Osaka 565-0871, Japan
[2]Laboratory of Hepatocyte Differentiation, National Institute of Biomedical Innovation, Osaka 567-0085, Japan
[3]iPS Cell-Based Research Project on Hepatic Toxicity and Metabolism, Graduate School of Pharmaceutical Sciences, Osaka University, Osaka 565-0871, Japan
[4]Laboratory of Stem Cell Regulation, National Institute of Biomedical Innovation, Osaka 567-0085, Japan
[5]Pharmaceutical Research and Technology Institute, Kinki University, Osaka 577-8502, Japan
[6]The Center for Advanced Medical Engineering and Informatics, Osaka University, Osaka 565-0871, Japan
*Correspondence: mizuguch@phs.osaka-u.ac.jp
http://dx.doi.org/10.1016/j.stemcr.2013.08.006

SUMMARY

The establishment of self-renewing hepatoblast-like cells (HBCs) from human pluripotent stem cells (PSCs) would realize a stable supply of hepatocyte-like cells for medical applications. However, the functional characterization of human PSC-derived HBCs was not enough. To purify and expand human PSC-derived HBCs, human PSC-derived HBCs were cultured on dishes coated with various types of human recombinant laminins (LN). Human PSC-derived HBCs attached to human laminin-111 (LN111)-coated dish via integrin alpha 6 and beta 1 and were purified and expanded by culturing on the LN111-coated dish, but not by culturing on dishes coated with other laminin isoforms. By culturing on the LN111-coated dish, human PSC-derived HBCs were maintained for more than 3 months and had the ability to differentiate into both hepatocyte-like cells and cholangiocyte-like cells. These expandable human PSC-derived HBCs would be manageable tools for drug screening, experimental platforms to elucidate mechanisms of hepatoblasts, and cell sources for hepatic regenerative therapy.

INTRODUCTION

Human embryonic stem cells (hESCs) and human induced pluripotent stem cells (hiPSCs) have the ability to self-replicate and to differentiate into all types of body cells including hepatoblasts and hepatocytes. Although cryopreserved primary human hepatocytes are useful in drug screening and liver cell transplantation, they rapidly lose their functions (such as drug metabolism capacity) and hardly proliferate in in vitro culture systems. On the other hand, human hepatic stem cells from fetal and postnatal human liver are able to self-replicate and able to differentiate into hepatocytes (Schmelzer et al., 2007; Zhang et al., 2008). However, the source of human hepatic stem cells is limited, and these cells are not available commercially. Therefore, the human pluripotent stem cell (hPSC)-derived hepatoblast-like cells (HBCs), which have potential to differentiate into the hepatocyte-like cells, would be an attractive cell source to provide abundant hepatocyte-like cells for drug screening and liver cell transplantation.

Because expandable and multipotent hepatoblasts or hepatic stem cells are of value, suitable culture conditions for the maintenance of hepatoblasts or hepatic stem cells obtained from fetal or adult mouse liver were developed (Kamiya et al., 2009; Tanimizu et al., 2004). Soluble factors, such as hepatocyte growth factor (HGF) and epidermal growth factor (EGF), are known to support the proliferation

of mouse hepatic stem cells and hepatoblast (Kamiya et al., 2009; Tanimizu et al., 2004). Extracellular matrix (ECM) also affects the maintenance of hepatoblasts or hepatic stem cells. Laminin can maintain the character of mouse hepatoblasts (Dlk1-positive cells) (Tanimizu et al., 2004). However, the methodology for maintaining HBCs differentiated from hPSCs has not been well investigated. Zhao et al. (2009) have reported that hESC-derived hepatoblast-like cells (sorted N-cadherin-positive cells were used) could be maintained on STO feeder cells. Although a culture system using STO feeder cells for the maintenance of hepatoblast-like cells might be useful, there are two problems. The first problem is that N-cadherin is not a specific marker for human hepatoblasts. N-cadherin is also expressed in hESC-derived mesendoderm cells and definitive endoderm (DE) cells (Sumi et al., 2008). The second problem is that residual undifferentiated cells could be maintained on STO feeder cells. Therefore, their culture condition cannot rule out the possibility of the proliferation of residual undifferentiated cells. Because it is known that hPSC-derived cells have the potential to form teratomas in the host, the production of safer hepatocyte-like cells or hepatoblast-like cells has been required. Therefore, we decided to purify hPSC-derived HBCs, which can differentiate into mature hepatocyte-like cells, and then expand these cells.

In this study, we attempt to determine a suitable culture condition for the extensive expansion of HBCs derived

CrossMark

from hPSCs. We found that the HBCs derived from hPSCs can be maintained and proliferated on human laminin-111 (LN111)-coated dishes. To demonstrate that expandable, multipotent, and safe (i.e., devoid of residual undifferentiated cells) hPSC-derived HBCs could be maintained under our culture condition, the hPSC-derived HBCs were used for hepatic and biliary differentiation, colony assay, and transplantation into immunodeficient mice.

RESULTS

Human PSC-Derived Hepatoblast-like Cells Could Adhere onto Human LN111 via Integrin α6 and β1

The HBCs were generated from hPSCs (hESCs and hiPSCs) as described in Figure 1A (details of the characterization of hPSC-derived HBCs are described in Figure 3). Definitive endoderm differentiation of hPSCs was promoted by stage-specific transient transduction of FOXA2 in addition to the treatment with appropriate soluble factors (such as Activin A). Overexpression of FOXA2 is not necessary for establishing the hPSC-derived HBCs, but it is helpful for efficient generation of the hPSC-derived HBCs. On day 9, these hESC-derived populations contained two cell populations with distinct morphology (Figure 1B). One population resembled human hepatic stem cells that were isolated from human fetal liver (shown in red) (Schmelzer et al., 2007), whereas the other population resembled definitive endoderm cells (shown in green) (Hay et al., 2008). The population that resembled human hepatic stem cells was alpha-1-fetoprotein (AFP) positive, whereas the other population was AFP negative (Figure 1C, left). On day 9, the percentage of AFP-positive cells was approximately 80% (Figure 1C, right). To characterize these two cell populations (hESC-derived HBC and non-HBC [NHBC] populations), the colonies were manually isolated by using a pipette, and then the gene expression analysis was performed. The gene expression levels of *AFP, CD133, EpCAM, CK8,* and *CK18* in the hESC-derived HBCs were higher than those in the bulk population containing both hESC-derived HBCs and NHBCs (*CD133, EpCAM, CK8,* and *CK18* were named as pan-hepatoblast markers and are known to be strongly expressed in both human hepatic stem cells and hepatoblasts [Schmelzer et al., 2007; Zhang et al., 2008]) (Figure 1D). On the other hand, the gene expressions of *AFP, CD133, EpCAM, CK8,* and *CK18* in the hESC-derived NHBCs were hardly detected. The gene expression levels of DE, mesendoderm, and pluripotent markers in the hESC-derived NHBCs were higher than those in the hESC-derived HBCs, indicating that the hESC-derived NHBCs could remain in a more undifferentiated state than the hESC-derived HBCs (Figures S1A–S1C available online). These results suggest

that hepatoblast-like cells could be differentiated from hPSCs.

To purify the hESC-derived HBCs, these cells were plated onto dishes coated with various laminins. There are 15 different laminin isoforms in human tissues. Although laminin is known to be useful to sustain mouse hepatoblasts (Tanimizu et al., 2004), it remains unknown which human laminin isoform has the potential to purify and expand the HBCs. To identify a human laminin isoform that would be useful for purifying hESC-HBCs, the hESC-HBCs and -NHBCs were plated onto dishes coated with various types of commercially available human laminins (Figure 1E). The hESC-derived HBCs could more efficiently adhere onto the human LN111-coated dish compared with hESC-derived NHBCs or unseparated populations (containing both HBCs and NBCs). These data suggest that a hESC-derived HBC population can be purified from the unseparated populations by culturing on human LN111-coated dishes. Because integrins are known to be important molecules for cell adhesion to the ECM including laminins, we expected that certain types of integrins would allow selective adhesion of the hESC-derived HBCs to human LN111-coated dish. The gene expression levels of various integrins were examined (Figure 1F). Among the integrin α subunits, the gene expression level of *integrin α6* in the hESC-derived HBCs was significantly higher than that in the hESC-derived NHBCs. In contrast, among the integrin β subunits, the gene expression level of *integrin β1* was higher than those of *integrin β2* and *β3* in all cell populations. The hESC-derived HBCs, but not NHBCs, expressed both integrin α6 and β1 (Figure S1D). Almost all adhesion of the hESC-derived HBCs to a human LN111-coated dish was inhibited by both function-blocking antibodies to integrin α6 and β1 (Figure 1G). These results indicated that the hESC-derived HBCs could attach to a human LN111-coated dish via integrin α6 and β1.

The hPSC-Derived HBCs Could Be Proliferated and Maintained on a Human LN111-Coated Dish

To obtain the purified hESC-derived HBC population, the hESC-derived cells (day 9) were plated onto a human LN111-coated dish, and then unattached cells were removed at 15 min after plating (Figure 2A). Among various laminins, only human LN111 could proliferate (Figure 2B) and purify (Figure 2C) the AFP-positive population in the presence of HGF and EGF. During culture on the human LN111-coated dish, the morphology of the hESC-derived HBCs gradually changed into that of human hepatoblasts (Figure S1E) (Schmelzer et al., 2007). Therefore, the characteristics of hESC-derived HBCs might be changed by culturing on a human LN111-coated dish (details of the characterization of the hESC-derived HBCs are described in Figure 3). After culturing on a human LN111-coated
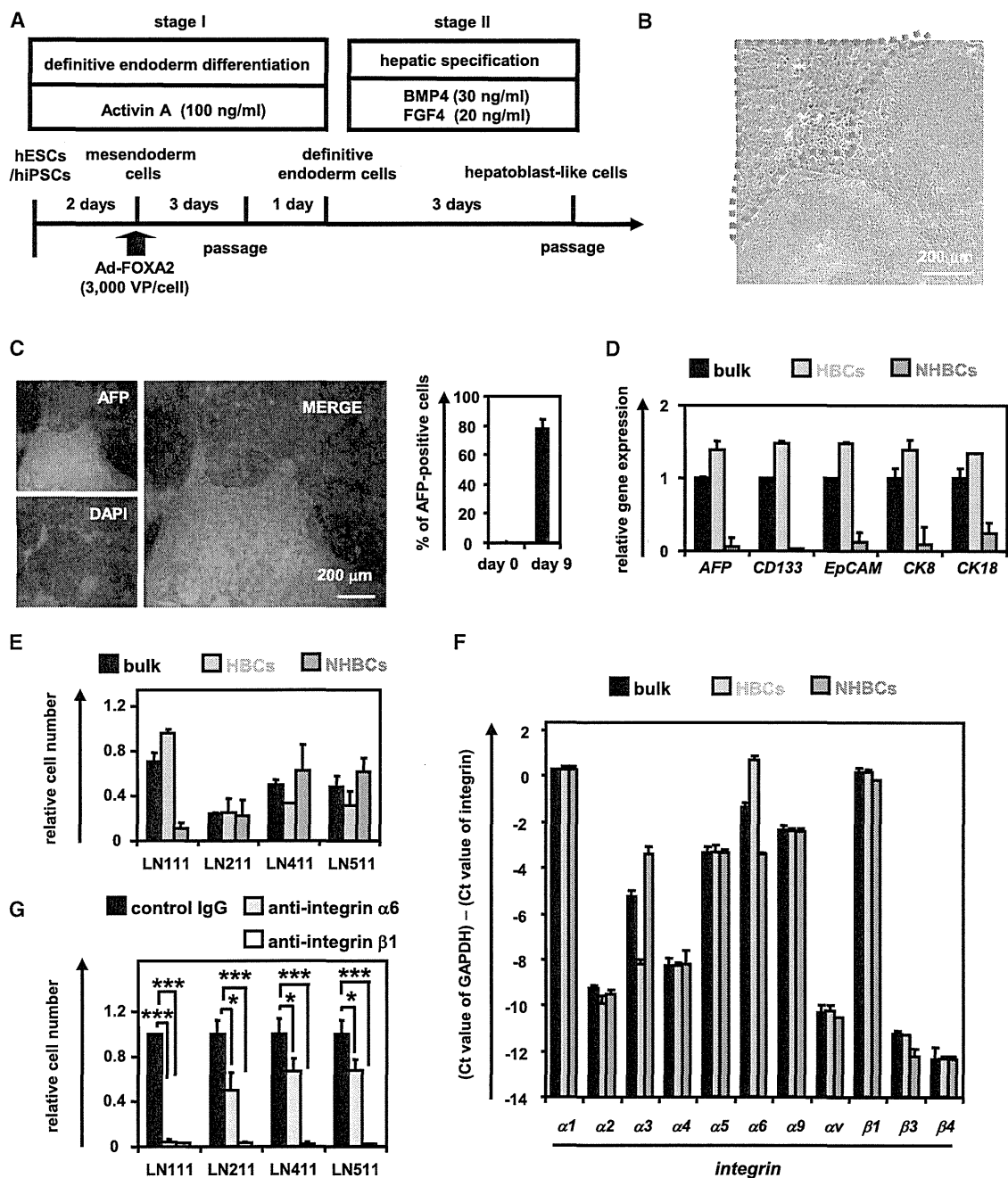
Figure 1. The Human ESC-Derived HBCs Selectively Attached to a Human LN111-Coated Dish via Integrin α6 and β1

(A) The procedure for the differentiation of hESCs (H9) into hepatoblast-like cells (HBCs) is presented schematically. Details are described in the Experimental Procedures.

(B) Phase-contrast micrographs of the hESC-derived HBCs (red) and non-HBCs (NHBCs) (green) are shown.

(C) The hESC-derived cells (day 9) were subjected to immunostaining with anti-AFP (red) antibodies. The percentage of AFP-positive cells was examined on day 0 or 9 by using FACS analysis. Data represent the mean ± SD from ten independent experiments. Cells on "day 0" and "day 9" were compared using Student's t test (p < 0.01).

(D) On day 9, the hESC-derived HBCs and NHBCs were manually picked, and the gene expression levels of AFP and pan-hepatoblast markers (CD133, EpCAM, CK8, and CK18) were measured by real-time RT-PCR. The gene expression levels of AFP and pan-hepatoblast markers in the hESC-derived cells (day 9; bulk) were taken as 1.0. Data represent the mean ± SD from four independent experiments. The gene expression levels in the HBCs were significantly different among the three groups (bulk, HBCs, and NHBCs) based on analysis with one-way ANOVA followed by Bonferroni post hoc tests (p < 0.05).

(legend continued on next page)

dish for a week, almost all of the cells were still AFP positive (Figures 2C and 2D). To characterize the cells cultured on various types of human laminins for 7 days, the gene expression levels of *AFP* and pan-hepatoblast (*CD133, CK8, CK18,* and *EpCAM*) markers were examined on day 16 (Figure 2E). The gene expression levels of *AFP* and pan-hepatoblast markers in the hESC-derived HBCs P1 (HBCs passaged once) did not change as compared with those of the hESC-derived HBCs (day 9; HBC P0) (the definitions of HBC P0, P1, P10, and clone in the present study are shown in Figure S3). The gene expression levels of mature hepatocyte and cholangiocyte markers in the hESC-derived HBC P1 did not change as compared with those of the hESC-derived HBC P0 (day 9) (Figure S1F). These results suggest that the characteristics of the hESC-derived HBC P1 are similar to those of the hESC-derived HBC P0, although their morphologies are quite different from each other. Interestingly, the gene expression levels of mature cholangiocyte markers in the cells cultured on human LN411- or 511-coated dishes were upregulated as compared with those of the hESC-derived HBC P0 (day 9) (Figure S1F), suggesting that human LN411 and 511 might promote biliary differentiation. Importantly, both hESC-derived HBCs and hiPSC-derived HBCs could extensively proliferate on a human LN111-coated dish for more than 15 passages (Figure 2F) in the presence of HGF and EGF. Doubling times of hESC (H9)-derived HBCs and hiPSC (Dotcom)-derived HBCs were approximately 78 and 67 hr, respectively. Almost all of the populations cultured on a human LN111-coated dish were AFP positive (Figure 2G). Taken together, these results suggested that the hPSC-derived HBCs would proliferate and be maintained on a human LN111-coated dish.

Characterization of the hESC-Derived HBCs

To characterize the hESC-derived HBCs, the gene expression profiles in the hESC-derived purified HBCs (HBC P0), short-term cultured HBCs (HBCs passaged once [HBC P1]), and long-term cultured HBC (HBCs passaged ten times [HBC P10]) were examined. The hESC-derived HBCs were AFP positive (Figure 3A). Although the hESC-

derived HBC P0 were negative for ALB, CK7, and CK19, the hESC-derived HBC P1 and P10 were positive for these genes (Figure 3A). Both integrin α6 and β1 (receptors of LN111) were strongly expressed in the hESC-derived HBC P0, P1, and P10 (Figure 3B). The gene expression levels of human hepatic stem cell markers (*N-CAM* and *Claudin 3* [Schmelzer et al., 2007]; these are not expressed in human hepatoblasts) in the hESC-derived HBC P0 were higher than those of the hESC-derived HBC P1 and P10 (Figure 3C). However, the gene expression level of *CK19* in the hESC-derived HBC P0 was lower than that of the hESC-derived HBC P1 and P10. The gene expression levels of pan-hepatoblast markers in the hESC-derived HBC P0 were similar to those of the hESC-derived HBC P1 and P10 (Figure 3D). The gene expression levels of human hepatoblast markers (*ALB, CYP3A7,* and *I-CAM* (Schmelzer et al., 2007), none of which were expressed in human hepatic stem cells) in the hESC-derived HBC P1 and P10 were higher than those of the hESC-derived HBC P0 (Figure 3E). However, the AFP expression level in the hESC-derived HBC P0 was similar to that of the hESC-derived HBC P1 and P10. Because the gene expression levels of mature hepatocyte and cholangiocyte markers in the hESC-derived HBC P1 and P10 were not increased as compared with those in the hESC-derived HBC P0 (Figure 3F), the hESC-derived HBC P1 and P10 were not segregated into either of the hepatic and biliary lineages. We also examined the gene expression levels of hepatoblast markers, which have been reported only in mice and not in humans (Figure 3G). The characteristics of the hPSC-derived HBCs are summarized in Figure S3. In addition, hESC-derived HBC P0 and HBC P10 showed normal karyotypes (Figure S2A). Therefore, the genetic stability of the HBCs was confirmed throughout the maintenance period. Taken together, these results suggest that the hESC-derived HBC P0 resemble human hepatic stem cells and the hESC-derived HBC P1 and P10 resemble human hepatoblasts, although some gene expression patterns in the hESC-derived HBCs differ from those in human hepatic stem cells and human hepatoblasts, respectively.

(E) The hESC-derived cells (day 9; bulk), HBCs, and NHBCs were plated onto human LN111-, 211-, 411-, or 511-coated dishes, and the attached cells were counted at 60 min after plating. The cell number that was initially plated was taken as 1.0. Data represent the mean ± SD from four independent experiments. The number of attached HBCs on LN111-coated dishes were significantly different among three groups (bulk, HBCs, and NHBCs) based on analysis with one-way ANOVA followed by Bonferroni post hoc tests (p < 0.05).

(F) The gene expression levels of the indicated integrins were measured in the hESC-derived cells (day 9; bulk), HBCs, and NHBCs by real-time RT-PCR. Data represent the mean ± SD from four independent experiments. The gene expression levels of *integrin α3* and *α6* in the HBCs were significantly different among three groups (bulk, HBCs, and NHBCs) based on analysis with one-way ANOVA followed by Bonferroni post hoc tests (p < 0.05).

(G) The adhesion of the hESC-derived HBCs to human LN111-, 211-, 411-, or 511-coated dishes was examined by using the indicated integrin antibodies. IgG antibodies were used as a control for uninhibited cell adhesion. The number of attached cells was estimated at 60 min after plating. The cell number in the control IgG-treated group was taken as 1.0. Data represent the mean ± SD from three independent experiments. "Control IgG" and "anti-integrin α6 or integrin β1" were compared using Student's t test. *p < 0.05; ***p < 0.001. See also Figure S1 and Tables S2–S5.
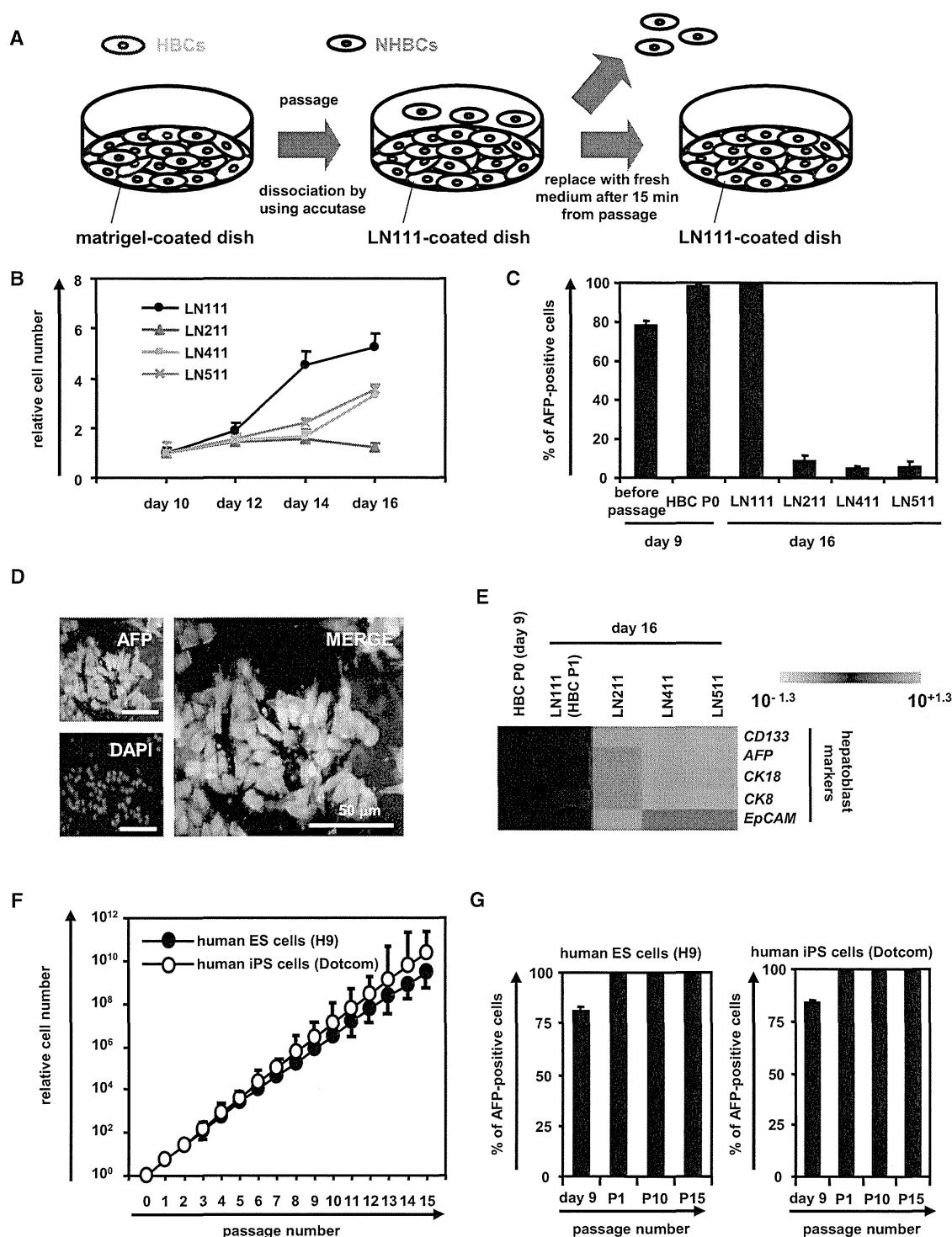
Figure 2. The hESC-Derived HBCs Could Be Proliferated and Maintained on a Human LN111-Coated Dish
(A) The hESC (H9)-derived cells (day 9) were plated onto a human LN111-coated dish. At 15 min after plating, the unattached cells were removed.
(B) The hESC (H9)-derived cells (day 9) were plated onto a human LN111, 211, 411, or 511-coated dish, and then the cell number were counted on days 10, 12, 14, and 16. The cell number on day 10 was taken as 1.0. Data represent the mean ± SD from three independent experiments. "LN111" was significantly different among four groups (LN111, 211, 411, and 511) on day 14 and 16 based on analysis with one-way ANOVA followed by Bonferroni post hoc tests (p < 0.05).

(legend continued on next page)

In order to examine whether the hESC-derived HBC P0 have the potential to proliferate clonally on various types of human laminins, single HBCs were plated on separate wells of a human LN111-coated 96-well plate at a low density (one cell per one well) (Table S1). Single cells that attached to the human LN111-coated dish were AFP positive and HNF4α positive (Figure S2B). At 7 days after plating, the hESC-derived HBC colonies (albumin [ALB]- and cytokeratin 7 [CK7] double positive) (a representative colony is shown in Figure S2C) were efficiently generated from the hESC-derived HBC P0 on a LN111-coated dish. Taken together, these results showed that the hESC-derived HBCs could be generated from both the hESC-derived HBC P0 population and the single hESC-derived HBC P0.

The hPSC-Derived HBCs Could Differentiate into Both Hepatic and Biliary Lineages In Vitro

To examine whether the hESC-derived HBCs have the potential to differentiate into both hepatic and biliary lineages, first, these cells were differentiated into hepatocyte-like cells as described in Figure 4A. After 2 weeks of hepatic differentiation, almost all of the cells were polygonal in shape (Figure 4B) and were CYP3A4, αAT, and ALB positive (Figure 4C). The gene expression levels of mature hepatocyte markers in the HBC P0-, HBC P10-, or HBC clone-derived hepatocyte-like cells were higher than those in the cells that had not undergone hepatic differentiation (Figure 4D), although the gene expression levels of mature cholangiocyte markers in these cells did not change (Figure 4E). The ASGR1-positive cells in the HBC P0-, HBC P10-, and HBC clone-derived population accounted for approximately 60%, 90%, and 90% of the total, respectively (Figure 4F). The HBC P0-, HBC P10-, or HBC clone-derived hepatocyte-like cells had the ability to produce ALB (Figure 4G, left) and urea (Figure 4G, right). Next, the hESC-derived HBCs were differentiated into cholangiocyte-like cells as described in Figure 4H. After 2 weeks of biliary differentiation, tubular structures (Fig-ure 4I) that were CK7 positive (Figure 4J) were observed. Although the gene expression levels of mature hepatocyte markers (Figure 4K) in the HBC P0-, HBC P10-, or HBC clone-derived cholangiocyte-like cells did not change, the gene expression levels of mature cholangiocyte markers (Figure 4L) in these cells were higher than those in the cells that had not undergone differentiation. Similar results were obtained by using another hESC line (H1) and hiPSC line (Dotcom) (Figure S4). Moreover, HBC-derived hepatocyte-like cells exhibited CYP metabolism capacity (Figure S5A) and a functional urea cycle that could response to ammonia (Figure S5B) and were considered to have potential to be applied in the prediction of drug-induced hepatotoxicity (Figure S5C). Taken together, these results indicated that the hPSC-derived HBCs have the ability to differentiate into both hepatic and biliary lineages in vitro.

In Vivo Cell Transplantation Assays of the hPSC-Derived HBCs

To examine whether the hESC-derived HBCs could be used for hepatocyte transplantation, these cells were transplanted into CCl4-treated immunodeficient mice as shown in Figure 5A. The hepatocyte functionality of the hESC-derived HBC P0 or HBC P10 was assessed by measuring secreted human ALB levels in the recipient mice (Figure 5B). Although human ALB was detected in the mice that were transplanted with the hESC-derived HBC P0 or HBC P10, it was not detected in the mice that were not transplanted with these cells. The ALB-positive cells were observed in mice transplanted with the hESC-derived HBC P0 or HBC P10 (Figure 5C). Most of the ALB-positive cells in mice transplanted with the hESC-derived HBC P10 were AFP negative (Figure 5D), indicating that transplanted hESC-derived HBCs were differentiated into mature hepatocyte-like cells (some of them were binuclear [Figure 5E, white arrows]). These results demonstrated that hESC-derived HBCs have the potential to be applied for hepatocyte transplantation.
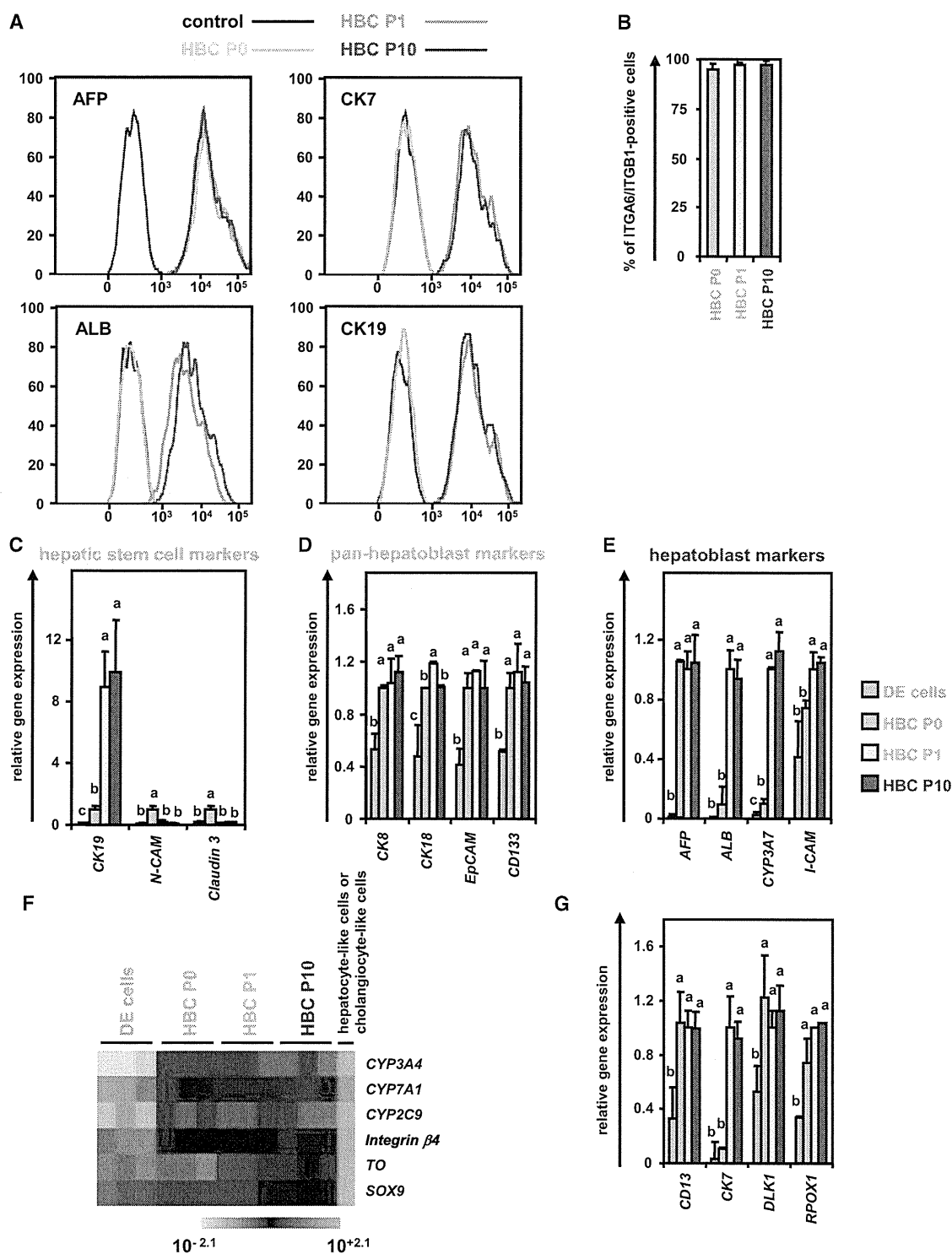

(C) The hESC-derived cells (day 9) were plated onto a human LN111, 211, 411, or 511-coated dish. The percentage of AFP-positive cells was examined by using FACS analysis on day 9 (before passage and after passage [HBC P0]) or day 16. Data represent the mean ± SD from three independent experiments.

(D) The hESC-derived cells cultured on a human LN111-coated dish for 7 days were subjected to immunostaining with anti-AFP (green) antibodies.

(E) The hESC-derived cells (day 9) were plated onto human LN111, 211, 411, or 511-coated dishes. The gene expression levels of AFP and pan-hepatoblast markers (CD133, EpCAM, CK8, and, CK18) were measured by real-time RT-PCR on day 16. The gene expression levels in the hESC-derived HBCs (the LN111-attached cells were collected at 15 min after plating) were taken as 1.0.

(F) The HBCs derived from hESCs (H9) or hiPSCs (Dotcom) were cultured and cell growth was analyzed by obtaining a cell count at each passage. Data represent the mean ± SD from three independent experiments.

(G) The percentage of AFP-positive cells was examined by using FACS analysis on day 9 (before passage), P1 (HBCs passaged once), P10 (HBCs passaged ten times), and P15 (HBCs passaged 15 times). Data represent the mean ± SD from seven independent experiments.
See also Tables S2 and S3.

A

control ——— HBC P1 ---------

HBC P0 --------- HBC P10 ———

AFP / CK7 / ALB / CK19

B

% of ITGA6/ITGB1-positive cells

HBC P0 / HBC P1 / HBC P10

C hepatic stem cell markers

relative gene expression

CK19 / N-CAM / Claudin 3

D pan-hepatoblast markers

relative gene expression

CK8 / CK18 / EpCAM / CD133

E hepatoblast markers

relative gene expression

AFP / ALB / CYP3A7 / I-CAM

DE cells
HBC P0
HBC P1
HBC P10

F

DE cells / HBC P0 / HBC P1 / HBC P10 | hepatocyte-like cells or cholangiocyte-like cells

CYP3A4
CYP7A1
CYP2C9
Integrin β4
TO
SOX9

$10^{-2.1}$ $10^{+2.1}$

G

relative gene expression

CD13 / CK7 / DLK1 / RPOX1

Figure 3. The hESC-Derived HBCs Were Characterized

(A and B) The hESCs (H9) were differentiated according to Figure 1A and then passaged onto a human LN111-coated dish. The attached cells (hESC-derived HBCs [HBC P0]) were collected at 15 min after plating. The percentage of AFP-positive, ALB-positive, CK7-positive, CK19-positive (A), and integrin α6- and integrin β1-double positive (B) cells in the hESC-derived HBC P0, HBC P1 (HBCs passaged once), and HBC P10 (HBCs passaged ten times) populations was estimated by using FACS analysis. Data represent the mean ± SD from seven independent experiments.

(legend continued on next page)

DISCUSSION

The main purpose of this study was to establish and characterize expandable HBCs from hPSCs. First, we identified that human LN111 could support self-renewal and proliferation of hPSC-derived HBCs in the presence of HGF and EGF. Second, we showed that the hPSC-derived HBCs have the potential to segregate into both hepatic and biliary lineages, and to integrate into the mouse liver parenchyma.

We have demonstrated that the hPSC-derived HBCs could be maintained on a human LN111-coated dish in an integrin α6- and β1-dependent manner (Figure 1). It is known that undifferentiated hPSCs could be maintained on a human LN511-coated dish but not on a human LN111-coated dish (Rodin et al., 2010). This might suggest that human LN111 has the potential not only to selectively maintain HBCs, but also to eliminate residual undifferentiated cells. Our hepatoblast-like cells could efficiently proliferate for more than 3 months on a human LN111-coated dish (Figure 2). In the human liver development (during 5–10 weeks gestation), laminin is observed in both the perisinusoidal space and portal tracts (Couvelard et al., 1998). The expression of laminin is localized around the periportal biliary trees during the later stage of liver development (Couvelard et al., 1998). Hepatic stem cells reside around the hepatic portal area (Clément et al., 1988). It is also known that laminin is accumulated around oval cells although laminin is not expressed around quiescent mature hepatocytes (Paku et al., 2001). These facts suggest that laminin plays an important role in the maintenance and proliferation of hepatoblasts.

The hPSC-derived HBC P10 and clone were positive for hepatoblast markers (AFP, ALB, CYP3A7, and I-CAM), but negative for hepatic stem cell markers (N-CAM and Claudin 3) (Figure 3) (Schmelzer et al., 2007). Although the hPSC-derived HBCs were able to expand on human LN111-coated dish, Schmelzer et al. showed that human hepatoblasts do not proliferate under a monolayer culture condition, but human hepatic stem cells could self-replicate for more than 6 months (Schmelzer et al., 2007). Although further investigations of the hepatoblast characteristics in the hPSC-derived HBCs will be needed in the future, the results in the present study suggest that the characteristics of hPSC-derived HBCs expanded on human LN111-coated dishes were similar to those in human hepatoblasts isolated from the human liver (Schmelzer et al., 2007; Zhang et al., 2008).

The hPSC-derived HBCs had the ability to integrate into the mouse liver parenchyma (Figure 5), in the manner of human hepatic stem cells or hepatoblasts (Schmelzer et al., 2007). The human ALB serum levels (approximately 20–70 ng/ml) in mice transplanted with the hESC-derived HBC P0 or HBC P10 were comparable to those in the previous paper in which the hESC-derived definitive endoderm cells, hepatoblasts, and hepatocyte-like cells were transplanted into mice (Liu et al., 2011), but were lower than those of human liver chimeric mice (Tateno et al., 2004). Human ALB serum levels would increase if more suitable host mice, such as urokinase plasminogen activator-SCID mice were used (Tateno et al., 2004).

In this study, we have developed a technology for the maintenance and proliferation of hPSC-derived HBCs by using human LN111. To transplant these cells for purposes of regenerative medicine, a xeno-free culture condition for hPSC-derived HBCs must be developed in the future. It is hoped that the hPSC-derived HBCs and their derivatives will be helpful in various medical applications, such as drug screening and regenerative medicine.

EXPERIMENTAL PROCEDURES

hESC and hiPSC Culture

The hESC lines (H1 [WA01] and H9 [WA09] [WiCell Research Institute]) and the hiPSC line, Dotcom (JCRB number: JCRB1327) (Makino et al., 2009; Nagata et al., 2009), were maintained on a feeder layer of mitomycin-C-treated mouse embryonic fibroblasts (Millipore) with ReproStem medium (ReproCELL) supplemented with 5 and 10 ng/ml fibroblast growth factor 2 (FGF2) (Katayama Kagaku Kogyo), respectively. H1 and H9 were used following the Guidelines for Derivation and Utilization of Human Embryonic Stem Cells of the Ministry of Education, Culture, Sports, Science and Technology of Japan, and, furthermore, the study was approved by an independent ethics committee.

In Vitro Hepatoblast Differentiation

The differentiation protocol for the induction of definitive endoderm cells and hepatoblasts was based on our previous report with some modifications (Inamura et al., 2011; Takayama et al., 2012a, 2012b, 2013). In mesendoderm differentiation, hESCs/iPSCs were

---

(C–F) The gene expression levels of hepatic stem cell markers (C), pan-hepatoblast markers (D), hepatoblast markers (E), and mature hepatocyte (*CYP3A4*, *7A1*, *2C9*, and *TO*) or cholangiocyte markers (*integrin β4* and *SOX9*) (F) were measured in the definitive endoderm cells, HBC P0, HBC P1, or HBC P10 by real-time RT-PCR.

(G) The gene expression levels of *CD13*, *CK7*, *DLK1*, and *PROX1* were measured in the hESC-derived definitive endoderm cells, HBC P0, HBC P1, or HBC P10 by real-time RT-PCR. Data represent the mean ± SD from three independent experiments. Statistical significance was evaluated by ANOVA followed by Bonferroni post hoc tests to compare four groups (DE cells, HBC P0, HBC P1, and HBC P10). Groups that do not share the same letter are significantly different from each other ($p < 0.05$). DE, definitive endoderm cells.
See also Figures S2 and S3 and Tables S2–S4.
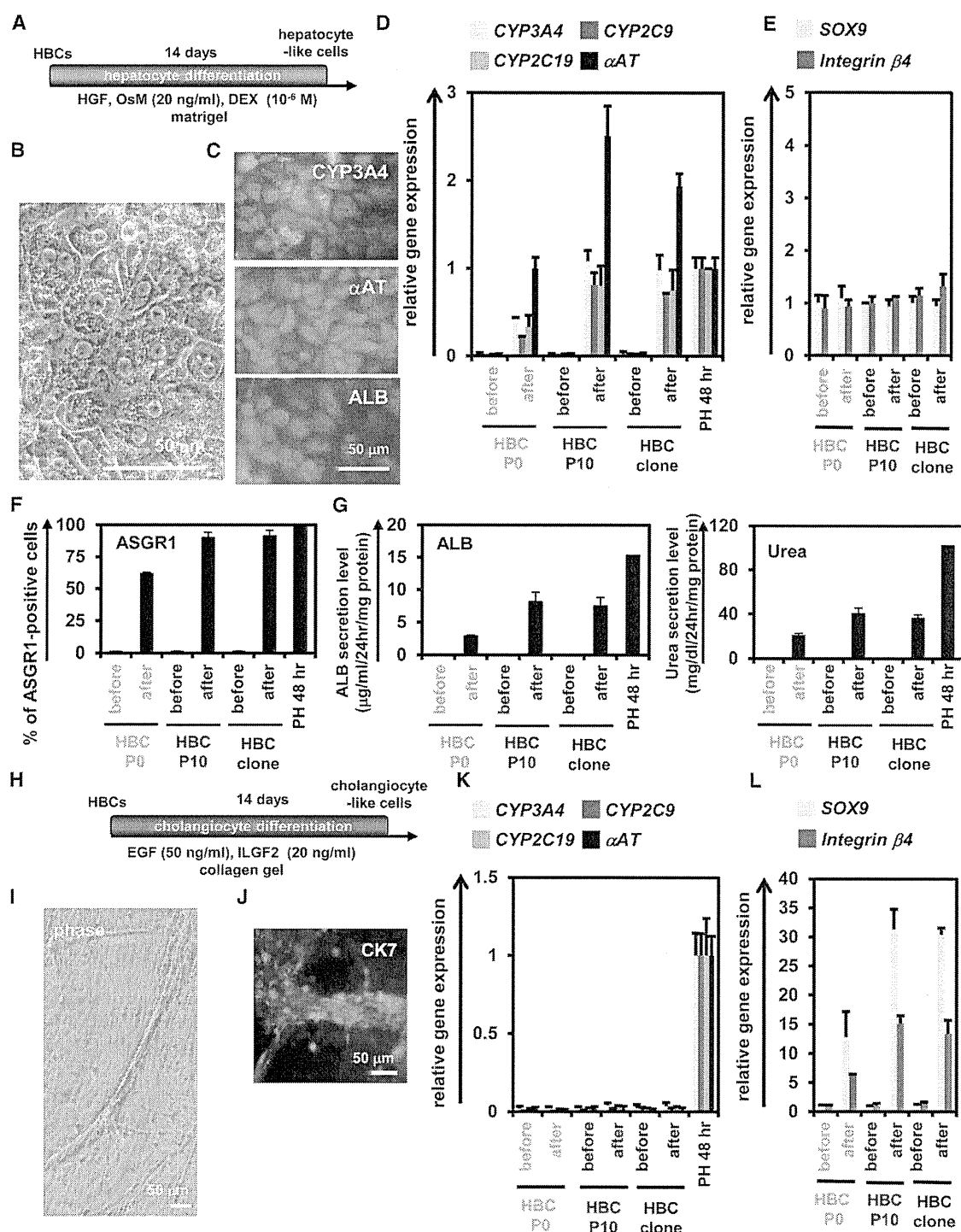
Figure 4. The hESC-Derived HBCs Could Differentiate into Both Hepatic and Biliary Lineages

(A) The procedure for differentiation of the hESC (H9)-derived HBC P0, HBC P10, or HBC clone into the hepatocyte-like cells is presented schematically. Details are described in Experimental Procedures.

(B) Phase-contrast micrographs of the HBC P10-derived hepatocyte-like cells are shown.

(C) The HBC P10-derived hepatocyte-like cells were subjected to immunostaining with anti-CYP3A4 (green), anti-αAT (red), and anti-ALB (red) antibodies.

(D and E) The gene expression levels of hepatocyte (D) or cholangiocyte (E) markers in HBC P0-, HBC P10-, or HBC clone-derived hepatocyte-like cells were measured by real-time RT-PCR after 14 days of hepatocyte differentiation. In (D), the gene expression levels in

(legend continued on next page)

cultured for 2 days on Matrigel (BD Biosciences) in differentiation hESF-DIF medium that contains 100 ng/ml Activin A (R&D Systems) (hESF-DIF medium was purchased from Cell Science & Technology Institute; differentiation hESF-DIF medium was supplemented with 10 μg/ml human recombinant insulin, 5 μg/ml human apotransferrin, 10 μM 2-mercaptoethanol, 10 μM ethanolamine, 10 μM sodium selenite, and 0.5 mg/ml bovine fatty acid free serum albumin [all from Sigma]). To generate definitive endoderm cells, the mes-endoderm cells (day 2) were transduced with 3,000 vector particle (VP)/cell of FOXA2-expressing adenovirus vectors (Ad-FOXA2) for 1.5 hr and cultured until day 6 on Matrigel in differentiation hESF-DIF medium supplemented with 100 ng/ml Activin A. For induction of hepatoblasts, the definitive endoderm cells were cultured for 3 days on a Matrigel in differentiation hESF-DIF medium supplemented with 30 ng/ml bone morphogenetic protein 4 (BMP4) (R&D Systems) and 20 ng/ml FGF4 (R&D Systems).

Establishment and Maintenance of the hPSC-Derived HBCs

The hPSC-derived HBCs were first purified from the hPSC-derived cells (day 9) by selecting attached cells on a human recombinant LN111 (BioLamina)-coated dish at 15 min after plating. The hPSC-derived HBCs were cultured on a human LN111-coated dish (2.0×10^4 cells/cm^2) in maintenance DMEM/F12 medium (DMEM/F12 medium [Invitrogen] was supplemented with 10% FBS, 1 × insulin/transferrin/selenium, 10 mM nicotinamide, 10^{-7} M dexamethasone (DEX) (Sigma), 20 mM HEPES, 25 mM NaHCO$_3$, 2 mM L-glutamine, penicillin/streptomycin, 40 ng/ml hepatocyte growth factor [HGF] [R&D Systems] and 20 ng/ml epidermal growth factors [EGF] [R&D Systems]). The medium was refreshed every day. The hPSC-derived HBCs were dissociated with Accutase (Millipore) into single cells and subcultured every 6 or 7 days.

Establishment and Maintenance of a Single hPSC-Derived HBC

For single-cell culture, the single HBC was plated to separate well of human LN111-coated 96-well plate in maintenance DMEM/F12

medium supplemented with 25 μM Y-27632 (ROCK inhibitor) (Millipore), and then colonies derived from a single cell were manually picked up and cultured as well as HBCs (these cells were designated the HBC clone).

In Vitro Hepatocyte and Cholangiocyte Differentiation

To induce hepatocyte differentiation, the hPSC-derived HBC P0, HBC P10, and HBC clone were cultured for 14 days on a Matrigel-coated dish (7.5×10^4 cells/cm^2) in HCM (Lonza) supplemented with 20 ng/ml HGF, 20 ng/ml Oncostatin M (OsM) (R&D Systems), and 10^{-6} M DEX. To induce cholangiocyte differentiation, the hPSC-derived HBC P0, HBC P10, and HBC clone were cultured in collagen gel for 14 days. To establish collagen gel plates, 500 μl collagen gel solution (consisting of 400 μl type I-A Collagen (Nitta gelatin), 50 μl 10 × DMEM, and 50 μl of 200 mM HEPES buffer containing 2.2% NaHCO$_3$ and 0.05 M NaOH) was added to each well, and then the plates were incubated at 37°C for 30 min. The hPSC-derived HBC P0, HBC P10, and HBC clone (5×10^4 cells) were resuspended in 500 μl differentiation DMEM/F12 medium (differentiation DMEM/F12 medium was supplemented with 20 mM HEPES, 2 mM L-glutamine, 100 ng/ml EGF, and 40 ng/ml insulin-like growth factor 2 [ILGF2]), and then mixed with 500 μl of the collagen gel solution and plated onto the basal layer of collagen. After 30 min, 2 ml of differentiation DMEM/F12 medium was added to the well.

Ad Vectors

Ad vectors were constructed by an improved in vitro ligation method. The human EF-1α promoter-driven FOXA2-expressing Ad vectors (Ad-FOXA2) were constructed previously (Takayama et al., 2012b). All of Ad vectors contain a stretch of lysine residue (K7) peptides in the C-terminal region of the fiber knob for more efficient transduction of hESCs, hiPSCs, mesendoderm cells, and definitive endoderm cells, in which transfection efficiency was almost 100%, and purified as described previously (Inamura

---

PH 48 hr were taken as 1.0. In (E), the gene expression levels in HBC P10 (before differentiation) were taken as 1.0. Data represent the mean ± SD from three independent experiments. Student's t test indicated that gene expression levels of the hepatocyte markers in "after" were significantly higher than those in "before" (p < 0.01).

(F) The efficiency of hepatocyte differentiation was measured by estimating the percentage of ASGR1-positive cells using FACS analysis.

(G) The amounts of ALB (left) and urea (right) secretion were examined. Data represent the mean ± SD from three independent experiments. Student's t test indicated that the percentage of ASGR1-positive cells, the ALB secretion level, and urea secretion level in "after" were significantly higher than those in "before" (p < 0.01).

(H) The procedure for the differentiation of the hESC-derived HBC P0, HBC P10, or HBC clone into cholangiocyte-like cells is presented schematically. Details are described in Experimental Procedures.

(I) Phase-contrast micrographs of the HBC P10-derived cholangiocyte-like cells are shown.

(J) The HBC P10-derived cholangiocyte-like cells were subjected to immunostaining with anti-CK7 (red) antibodies.

(K and L) The gene expression levels of hepatocyte (K) or cholangiocyte (L) markers in the HBC P0-, HBC P10-, or HBC clone-derived cholangiocyte-like cells were measured by real-time RT-PCR after 14 days of cholangiocyte differentiation. In (K), the gene expression levels in PH 48 hr were taken as 1.0. In (L), the gene expression levels in HBC P10 (before cholangiocyte differentiation) were taken as 1.0. Data represent the mean ± SD from three independent experiments. Student's t test indicated that the gene expression levels of cholangiocyte markers in "after" were significantly higher than those in "before" (p < 0.01). "Before" indicates the HBCs before hepatocyte or cholangiocyte differentiation; "After" indicates the HBCs after hepatocyte or cholangiocyte differentiation.

See also Figures S4 and S5 and Tables S1–S4.
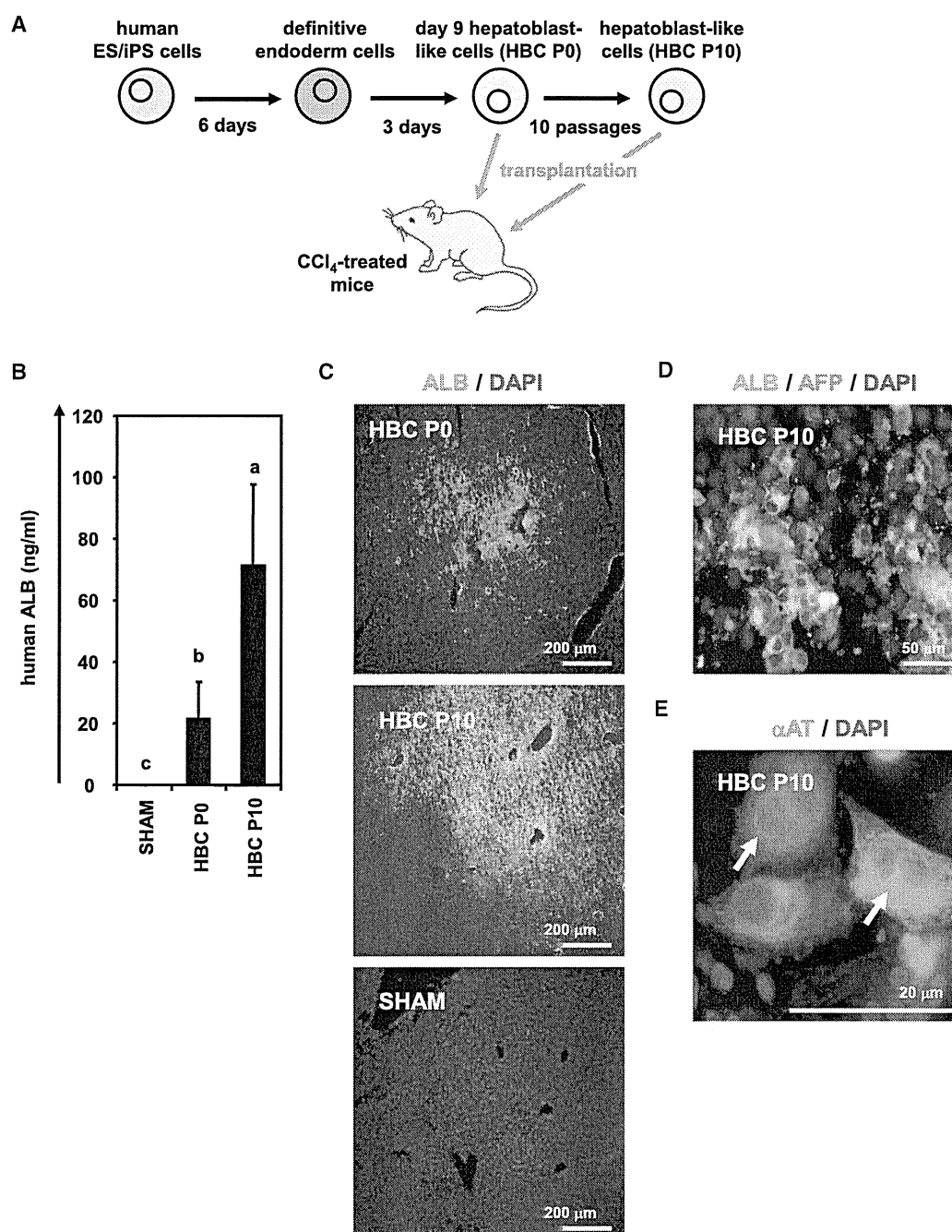
Figure 5. The hESC-Derived HBCs Were Integrated into the Mouse Liver Parenchyma

(A) The procedure for transplantation of the hESC (H9)-derived HBC P0 and HBC P10 into CCl_4 (4 ml/kg)-treated Rag2/IL2 receptor gamma double-knockout mice is presented schematically.

(B) The human ALB level in recipient mouse serum was measured at 2 weeks after transplantation. Data represent the mean ± SD from six to eight mice in each group. Statistical significance was evaluated by ANOVA followed by Bonferroni post hoc tests to compare all groups. Groups that do not share the same letter are significantly different from each other ($p < 0.05$).

(C) Expressions of the ALB (green) in the liver of transplanted mice were examined by immunohistochemistry at 2 weeks after transplantation.

(D and E) The expressions of AFP (red), ALB (green) (D), and αAT (red) (E) were examined by immunohistochemistry at 2 weeks after hESC-derived HBC P10 transplantation. White arrows show transplanted cells, which have double nuclei.

See also Tables S2 and S3.

et al., 2011; Takayama et al., 2011; Tashiro et al., 2010). The VP titer was determined by using a spectrophotometric method.

Flow Cytometry

Single-cell suspensions of the hPSC-derived cells were fixed with 4% paraformaldehyde (PFA) at 4°C for 10 min and then incubated with the primary antibody (described in Table S2), followed by the secondary antibody (described in Table S3). Control cells were incubated with anti-mouse, goat, or rabbit immunoglobulin (Ig) G antibodies (Santa Cruz Biotechnology) and then incubated with the secondary antibody. Flow cytometry analysis was performed using a fluorescence-activated cell sorting (FACS) LSR Fortessa flow cytometer (BD Biosciences). Cell sorting was performed using a FACS Aria (BD Biosciences).

RNA Isolation and RT-PCR

Total RNA was isolated from hPSCs and their derivatives using ISOGENE (Nippon Gene). cDNA was synthesized using 500 ng of total RNA with a Superscript VILO cDNA synthesis kit (Invitrogen). Real-time RT-PCR was performed with SYBR green PCR Master Mix (Applied Biosystems) using an Applied Biosystems StemOnePlus real-time PCR systems. Relative quantification was performed against a standard curve, and the values were normalized against the input determined for the housekeeping gene, glyceraldehyde 3-phosphate dehydrogenase. The primer sequences used in this study are described in Table S4. In addition, we confirmed that every beta integrin primer used in this manuscript showed a similar amplification efficacy (Table S5). The amplification efficiency was calculated from the slope of the standard curve according to the following formula: $e = 10^{(-1/slope)}-1$. Every beta integrin primer used in this manuscript showed a similar amplification efficacy.

Immunohistochemistry

The cells were fixed with 4% PFA for 15 min and then blocked with PBS containing 2% FBS, 2% bovine serum albumin (BSA), and 0.1% Triton X-100 (Wako Pure Chemicals Industries) for 1 hr. The cells were incubated with primary antibody (described in Table S2) at 4°C for overnight, followed by incubation with a secondary antibody (described in Table S3) at room temperature for 1 hr. Nuclei were counterstained with DAPI (blue).

ELISA

The hPSC-derived HBC P0, HBC P10, and HBC clone were differentiated into the hepatocyte-like cells as described in Figure 4A. The culture supernatants, which were incubated for 24 hr after fresh medium was added, were collected and analyzed for the amount of ALB secretion by ELISA. ELISA kits for ALB were purchased from Bethyl Laboratories. The amount of ALB secretion was calculated according to each standard followed by normalization to the protein content per well. The human ALB amount in mice serum was also examined by ELISA.

Transplantation of the hESC-Derived HBCs

The hESC-derived HBCs were dissociated using accutase and then suspended with maintenance DMEM/F12 medium without serum.

Eight- to 10-week-old Rag2/IL2Rg double-knockout mice were prepared. The hESC-derived HBCs (1×10^6 cells) were transplanted 24 hr after administration of CCl_4 (4 ml/kg) by intrasplenical injection. Recipient mouse liver and blood were harvested at 2 weeks after transplantation. The livers were fixed with 4% PFA and processed for immunohistochemistry. Human hepatocytes producing the ALB, AFP, and αAT protein were identified in mouse liver by an antibody specifically recognizing human but not mouse albumin. In addition, serum was extracted and subjected to ELISA analysis. All animal experiments were conducted in accordance with institutional guidelines.

Urea Secretion

The hPSC-derived HBC P0, HBC P10, and HBC clone were differentiated into hepatocyte-like cells as described in Figure 4A. The culture supernatants, which were incubated for 24 hr after fresh medium was added, were collected and analyzed for the amount of urea secretion. The urea measurement kits were purchased from BioAssay Systems. The amount of urea secretion was calculated according to each standard followed by normalization to the protein content per well. In Figure S5B, both the HBC-derived hepatocyte-like cells and primary human hepatocytes (PHs) (three lots of cryopreserved human hepatocytes were used), that were cultured for 48 hr after the cells were plated (PH 48 hr), were cultured in HCM (containing glutamine) or DMEM (not containing glutamine; Wako) in the presence or absence of 1 mM ammonium chloride (NH_4Cl, Wako) for 24 hr, and then the amount of urea secretion was measured.

Primary Human Hepatocytes

Three lots of cryopreserved human hepatocytes (lot Hu8072 [CellzDirect], HC2-14, and HC10-101 [Xenotech]) were used. The vials of hepatocytes were rapidly thawed in a shaking water bath at 37°C; the contents of the vial were emptied into prewarmed Cryopreserved Hepatocyte Recovery Medium (Gibco) and the suspension was centrifuged at 100 g for 10 min at room temperature. The hepatocytes were seeded at 1.25×10^5 cells/cm² in HCM (Lonza) containing 10% fetal calf serum (FCS) (Gibco) onto type I collagen-coated 12-well plates. The medium was replaced with hepatocyte culture medium containing 10% FCS 6 hr after seeding. The hepatocytes, which were cultured 48 hr after plating the cells, were used in the experiments.

Adhesion-Blocking Assay Using Integrin Antibody

Twelve-well plates were coated with human recombinant LN111, 211, 411, or 511 (all from BioLamina) and blocked by 1% heat-denatured BSA containing PBS. The hESC-derived single cells were incubated with function-blocking antibodies to integrin α6 and β1 (at the concentrations as recommended by the manufacturer) for 30 min, plated on a human LN111-coated 12-well dish, and allowed to adhere for 1 hr at 37°C. After unattached cells were removed, the remaining adherent cells were fixed for 20 min with 5% glutaraldehyde. The hESC-derived cells that had adhered to the wells were stained with 200 µl of 0.3% crystal violet (Wako) solution at room temperature for 15 min. Excess crystal violet was then removed, and the wells were washed three times. Fixed crystal violet was solubilized in 200 µl of 100% ethanol at room

temperature for 15 min. Cell viability was estimated by measuring the absorbance at 595 nm of each well using a microtiter plate reader (Sunrise, Tecan).

CYP Activity

To measure the CYP1A2, 2C9, and 3A4 activity of the cells, we performed lytic assays by using P450-GloTM CYP1A2, 2C9, and 3A4 Assay Kits (Promega), respectively. We measured the fluorescence activity with a luminometer (Lumat LB 9507; Berthold) according to the manufacturer's instructions. The CYP activity was normalized with the protein content per well.

Karyotyping

This experiment was carried out at Chromosome Science Labo.

Cell Viability Tests

Cell viability was assessed by using a WST-8 assay kit (Dojindo), and the results are presented in Figure S5C. After treatment with test compounds, such as acetaminophen (Wako) and troglitazone (Wako) for 24 hr, the cell viability was measured. The control cells were incubated in the absence of test compounds and were considered to have 100% viability value. Controls were treated with DMSO (final concentration 0.1%).

SUPPLEMENTAL INFORMATION

Supplemental Information includes five figures and five tables and can be found with this article online at http://dx.doi.org/10.1016/j.stemcr.2013.08.006.

REFERENCES

Clément, B., Rescan, P.Y., Baffet, G., Loréal, O., Lehry, D., Campion, J.P., and Guillouzo, A. (1988). Hepatocytes may produce laminin in fibrotic liver and in primary culture. Hepatology 8, 794–803.

Couvelard, A., Bringuier, A.F., Dauge, M.C., Nejjari, M., Darai, E., Benifla, J.L., Feldmann, G., Henin, D., and Scoazec, J.Y. (1998). Expression of integrins during liver organogenesis in humans. Hepatology 27, 839–847.

Hay, D.C., Zhao, D., Fletcher, J., Hewitt, Z.A., McLean, D., Urruti-coechea-Uriguen, A., Black, J.R., Elcombe, C., Ross, J.A., Wolf, R., and Cui, W. (2008). Efficient differentiation of hepatocytes from human embryonic stem cells exhibiting markers recapitulating liver development in vivo. Stem Cells 26, 894–902.

Inamura, M., Kawabata, K., Takayama, K., Tashiro, K., Sakurai, F., Katayama, K., Toyoda, M., Akutsu, H., Miyagawa, Y., Okita, H., et al. (2011). Efficient generation of hepatoblasts from human ES cells and iPS cells by transient overexpression of homeobox gene HEX. Mol. Ther. 19, 400–407.

Kamiya, A., Kakinuma, S., Yamazaki, Y., and Nakauchi, H. (2009). Enrichment and clonal culture of progenitor cells during mouse postnatal liver development in mice. Gastroenterology 137, 1114–1126.

Liu, H., Kim, Y., Sharkis, S., Marchionni, L., and Jang, Y.Y. (2011). In vivo liver regeneration potential of human induced pluripotent stem cells from diverse origins. Sci. Transl. Med. 3, 82ra39.

Makino, H., Toyoda, M., Matsumoto, K., Saito, H., Nishino, K., Fukawatase, Y., Machida, M., Akutsu, H., Uyama, T., Miyagawa, Y., et al. (2009). Mesenchymal to embryonic incomplete transition of human cells by chimeric OCT4/3 (POU5F1) with physiological co-activator EWS. Exp. Cell Res. 315, 2727–2740.

Nagata, S., Toyoda, M., Yamaguchi, S., Hirano, K., Makino, H., Nishino, K., Miyagawa, Y., Okita, H., Kiyokawa, N., Nakagawa, M., et al. (2009). Efficient reprogramming of human and mouse primary extra-embryonic cells to pluripotent stem cells. Genes Cells 14, 1395–1404.

Paku, S., Schnur, J., Nagy, P., and Thorgeirsson, S.S. (2001). Origin and structural evolution of the early proliferating oval cells in rat liver. Am. J. Pathol. 158, 1313–1323.

Rodin, S., Domogatskaya, A., Ström, S., Hansson, E.M., Chien, K.R., Inzunza, J., Hovatta, O., and Tryggvason, K. (2010). Long-term self-renewal of human pluripotent stem cells on human recombinant laminin-511. Nat. Biotechnol. 28, 611–615.

Schmelzer, E., Zhang, L., Bruce, A., Wauthier, E., Ludlow, J., Yao, H.L., Moss, N., Melhem, A., McClelland, R., Turner, W., et al. (2007). Human hepatic stem cells from fetal and postnatal donors. J. Exp. Med. 204, 1973–1987.

Sumi, T., Tsuneyoshi, N., Nakatsuji, N., and Suemori, H. (2008). Defining early lineage specification of human embryonic stem cells by the orchestrated balance of canonical Wnt/beta-catenin, Activin/Nodal and BMP signaling. Development 135, 2969–2979.

Takayama, K., Inamura, M., Kawabata, K., Tashiro, K., Katayama, K., Sakurai, F., Hayakawa, T., Furue, M.K., and Mizuguchi, H. (2011). Efficient and directive generation of two distinct endoderm lineages from human ESCs and iPSCs by differentiation stage-specific SOX17 transduction. PLoS ONE 6, e21780.

Takayama, K., Inamura, M., Kawabata, K., Katayama, K., Higuchi, M., Tashiro, K., Nonaka, A., Sakurai, F., Hayakawa, T., Furue, M.K., and Mizuguchi, H. (2012a). Efficient generation of functional hepatocytes from human embryonic stem cells and induced pluripotent stem cells by HNF4α transduction. Mol. Ther. 20, 127–137.

Takayama, K., Inamura, M., Kawabata, K., Sugawara, M., Kikuchi, K., Higuchi, M., Nagamoto, Y., Watanabe, H., Tashiro, K., Sakurai,

F., et al. (2012b). Generation of metabolically functioning hepatocytes from human pluripotent stem cells by FOXA2 and HNF1α transduction. J. Hepatol. *57*, 628–636.

Takayama, K., Kawabata, K., Nagamoto, Y., Kishimoto, K., Tashiro, K., Sakurai, F., Tachibana, M., Kanda, K., Hayakawa, T., Furue, M.K., and Mizuguchi, H. (2013). 3D spheroid culture of hESC/hiPSC-derived hepatocyte-like cells for drug toxicity testing. Biomaterials *34*, 1781–1789.

Tanimizu, N., Saito, H., Mostov, K., and Miyajima, A. (2004). Long-term culture of hepatic progenitors derived from mouse Dlk+ hepatoblasts. J. Cell Sci. *117*, 6425–6434.

Tashiro, K., Kawabata, K., Inamura, M., Takayama, K., Furukawa, N., Sakurai, F., Katayama, K., Hayakawa, T., Furue, M.K., and Mizuguchi, H. (2010). Adenovirus vector-mediated efficient transduc-tion into human embryonic and induced pluripotent stem cells. Cell Reprogram. *12*, 501–507.

Tateno, C., Yoshizane, Y., Saito, N., Kataoka, M., Utoh, R., Yamasaki, C., Tachibana, A., Soeno, Y., Asahina, K., Hino, H., et al. (2004). Near completely humanized liver in mice shows human-type metabolic responses to drugs. Am. J. Pathol. *165*, 901–912.

Zhang, L., Theise, N., Chua, M., and Reid, L.M. (2008). The stem cell niche of human livers: symmetry between development and regeneration. Hepatology *48*, 1598–1607.

Zhao, D., Chen, S., Cai, J., Guo, Y., Song, Z., Che, J., Liu, C., Wu, C., Ding, M., and Deng, H. (2009). Derivation and characterization of hepatic progenitor cells from human embryonic stem cells. PLoS ONE *4*, e6468.

THE COMPANY OF
Biologists

RESEARCH ARTICLE

CCAAT/enhancer binding protein-mediated regulation of TGFβ receptor 2 expression determines the hepatoblast fate decision

Kazuo Takayama[1,2,3], Kenji Kawabata[4], Yasuhito Nagamoto[1,2], Mitsuru Inamura[1], Kazuo Ohashi[5], Hiroko Okuno[1], Tomoko Yamaguchi[4], Katsuhisa Tashiro[4], Fuminori Sakurai[1], Takao Hayakawa[6], Teruo Okano[5], Miho Kusada Furue[7,8] and Hiroyuki Mizuguchi[1,2,3,9,*]

ABSTRACT

Human embryonic stem cells (hESCs) and their derivatives are expected to be used in drug discovery, regenerative medicine and the study of human embryogenesis. Because hepatocyte differentiation from hESCs has the potential to recapitulate human liver development *in vivo*, we employed this differentiation method to investigate the molecular mechanisms underlying human hepatocyte differentiation. A previous study has shown that a gradient of transforming growth factor beta (TGFβ) signaling is required to segregate hepatocyte and cholangiocyte lineages from hepatoblasts. Although CCAAT/enhancer binding proteins (c/EBPs) are known to be important transcription factors in liver development, the relationship between TGFβ signaling and c/EBP-mediated transcriptional regulation in the hepatoblast fate decision is not well known. To clarify this relationship, we examined whether c/EBPs could determine the hepatoblast fate decision via regulation of TGFβ receptor 2 (TGFBR2) expression in the hepatoblast-like cells differentiated from hESCs. We found that *TGFBR2* promoter activity was negatively regulated by c/EBPα and positively regulated by c/EBPβ. Moreover, c/EBPα overexpression could promote hepatocyte differentiation by suppressing TGFBR2 expression, whereas c/EBPβ overexpression could promote cholangiocyte differentiation by enhancing TGFBR2 expression. Our findings demonstrated that c/EBPα and c/EBPβ determine the lineage commitment of hepatoblasts by negatively and positively regulating the expression of a common target gene, *TGFBR2*, respectively.

KEY WORDS: Hepatoblasts, c/EBP, CEBP, Human ESCs

INTRODUCTION

Many animal models, such as chick, *Xenopus*, zebrafish and mouse, have been used to investigate the molecular mechanisms of liver development. Because many functions of the key molecules in liver

[1]Laboratory of Biochemistry and Molecular Biology, Graduate School of Pharmaceutical Sciences, Osaka University, Osaka 565-0871, Japan. [2]Laboratory of Hepatocyte Differentiation, National Institute of Biomedical Innovation, Osaka 567-0085, Japan. [3]iPS Cell-based Research Project on Hepatic Toxicity and Metabolism, Graduate School of Pharmaceutical Sciences, Osaka University, Osaka 565-0871, Japan. [4]Laboratory of Stem Cell Regulation, National Institute of Biomedical Innovation, Osaka 567-0085, Japan. [5]Institute of Advanced Biomedical Engineering and Science, Tokyo Women's Medical University, Tokyo 162-8666, Japan. [6]Pharmaceutical Research and Technology Institute, Kinki University, Osaka 577-8502, Japan. [7]Laboratory of Embryonic Stem Cell Cultures, Department of Disease Bioresources Research, National Institute of Biomedical Innovation, Osaka 567-0085, Japan. [8]Department of Embryonic Stem Cell Research, Field of Stem Cell Research, Institute for Frontier Medical Sciences, Kyoto University, Kyoto 606-8507, Japan. [9]The Center for Advanced Medical Engineering and Informatics, Osaka University, Osaka 565-0871, Japan.

*Author for correspondence (mizuguch@phs.osaka-u.ac.jp)

development are conserved in these species, studies on liver development in these animals can be highly informative with respect that in humans. However, some functions of important molecules in liver development might differ between human and other species. Although analysis using genetically modified mice has been successfully performed, it is not of course possible to perform genetic experiments to elucidate molecular mechanisms of liver development in human. Pluripotent stem cells, such as human embryonic stem cells (hESCs), are expected to overcome some of these problems in the study of human embryogenesis, including liver development, because the gene expression profiles of this model are similar to those in normal liver development (Agarwal et al., 2008; DeLaForest et al., 2011).

During liver development, hepatoblasts differentiate into hepatocytes and cholangiocytes. A previous study has shown that a high concentration of transforming growth factor beta (TGFβ) could give rise to cholangiocyte differentiation from hepatoblasts (Clotman et al., 2005). To transmit the TGFβ signaling, TGFβ receptor 2 (TGFBR2) has to be stimulated by TGFβ1, TGFβ2 or TGFβ3 (Kitisin et al., 2007). TGFβ binding to the extracellular domain of TGFBR2 induces a conformational change, resulting in the phosphorylation and activation of TGFBR1. TGFBR1 phosphorylates SMAD2 or SMAD3, which binds to SMAD4, and then the SMAD complexes move into the nucleus and function as transcription factors to express various kinds of differentiation-related genes (Kitisin et al., 2007). Although the function of TGFBR2 in regeneration of the adult liver has been thoroughly examined (Oe et al., 2004), the function of TGFBR2 in the hepatoblast fate decision has not been elucidated.

CCAAT/enhancer binding protein (c/EBP) transcription factors play decisive roles in the differentiation of various cell types, including hepatocytes (Tomizawa et al., 1998; Yamasaki et al., 2006). The analysis of *c/EBPα* (*Cebpa*) knockout mice has shown that many abnormal pseudoglandular structures, which co-express antigens specific for both hepatocytes and cholangiocytes, are present in the liver parenchyma (Tomizawa et al., 1998). These data demonstrated that c/EBPα plays an important role in hepatocyte differentiation. It is also known that the suppression of c/EBPα expression in periportal hepatoblasts stimulates cholangiocyte differentiation (Yamasaki et al., 2006). Although the function of c/EBPα in liver development is well known, the relationship between TGFβ signaling and c/EBPα-mediated transcriptional regulation in the hepatoblast fate decision is poorly understood. c/EBPβ is also known to be an important factor for liver function (Chen et al., 2000), although the function of c/EBPβ in the cell fate decision of hepatoblasts is not well known. c/EBPα and c/EBPβ bind to the same DNA binding site. However, the promoter activity of hepatocyte-specific genes, such as those encoding hepatocyte nuclear factor 6 (HNF6, also known as ONECUT1) and UGT2B1,

is positively regulated by c/EBPα but not c/EBPβ (Hansen et al., 1998; Plumb-Rudewiez et al., 2004), suggesting that the functions of c/EBPα and c/EBPβ in the hepatoblast fate decision might be different.

In the present study, we first examined the function of TGFBR2 in the hepatoblast fate decision using hESC-derived hepatoblast-like cells, which have the ability to self-replicate, differentiate into both hepatocyte and cholangiocyte lineages, and repopulate the liver of carbon tetrachloride (CCl₄)-treated immunodeficient mice. *In vitro* gain- and loss-of-function analyses and *in vivo* transplantation analysis were performed. Next, we investigated how TGFBR2 expression is regulated in the hepatoblast fate decision. Finally, we examined whether our findings could be reproduced in delta-like 1 homolog (Dlk1)-positive hepatoblasts obtained from the liver of E13.5 mice. To the best of our knowledge, this study provides the first evidence of c/EBP-mediated regulation of TGFBR2 expression in the human hepatoblast fate decision.

RESULTS

Hepatoblast-like cells are generated from hESCs

First, we investigated whether the hepatoblast-like cells (HBCs), which were differentiated from hESCs as described in supplementary material Fig. S1A, have similar characteristics to human hepatoblasts. We recently found that hESC-derived HBCs could be purified and maintained on human laminin 111 (LN111)-coated dishes (Takayama et al., 2013). The long-term cultured HBC population (HBCs passaged more than three times were used in this study) were nearly homogeneous and expressed human hepatoblast markers such as alpha-fetoprotein (AFP), albumin (ALB), cytokeratin 19 (CK19, also known as KRT19) and EPCAM (Schmelzer et al., 2007) (supplementary material Fig. S1B). In addition, most of the colonies observed on human LN111-coated plates were ALB and CK19 double positive, although a few colonies were ALB single positive, CK19 single positive, or ALB and CK19 double negative (supplementary material Fig. S1C). To examine the hepatocyte differentiation capacity of the HBCs *in vivo*, these cells were transplanted into CCl₄-treated immunodeficient mice. The hepatocyte functionality of the transplanted cells was assessed by measuring secreted human ALB levels in the recipient mice (supplementary material Fig. S1D). Human ALB serum was detected in the mice that were transplanted with the HBCs, but not in the control mice. These results demonstrated that the HBCs generated from hESCs have similar characteristics to human hepatoblasts and would therefore provide a valuable tool to investigate the mechanisms of human liver development. In the present study, HBCs generated from hESCs were used to elucidate the mechanisms of the hepatoblast fate decision.

TGFBR2 expression is decreased in hepatocyte differentiation but increased in cholangiocyte differentiation

The HBCs used in this study have the ability to differentiate into both hepatocyte-like cells [cytochrome P450 3A4 (CYP3A4) positive; Fig. 1B] and cholangiocyte-like cells (CK19 positive; Fig. 1C) (the protocols are described in Fig. 1A). Because the expression pattern of TGFBR2 during differentiation from hepatoblasts is not well known, we examined it in hepatocyte and cholangiocyte differentiation from HBCs. *TGFBR2* was downregulated during hepatocyte differentiation from HBCs (Fig. 1D), but upregulated in cholangiocyte differentiation from HBCs (Fig. 1E). After the HBCs were cultured on Matrigel, the cells were fractionated into three populations according to the level of TGFBR2 expression (TGFBR2-negative, -lo or -hi; Fig. 1F). The

HBC-derived TGFBR2-lo cells strongly expressed *αAT* and *CYP3A4* (hepatocyte markers), whereas the HBC-derived TGFBR2-hi cells strongly expressed *SOX9* and integrin β4 (*ITGB4*) (cholangiocyte markers). These data suggest that the TGFBR2 expression level is decreased in hepatic differentiation, but increased in biliary differentiation of the HBCs.

The cell fate decision of HBCs is regulated by TGFβ signals

To examine the function of TGFβ1, β2 and β3 (all of which are ligands of TGFBR2) in the hepatoblast fate decision, HBCs were cultured in medium containing TGFβ1, β2 or β3 (Fig. 2A,B). The expression levels of cholangiocyte marker genes were upregulated by addition of TGFβ1 or TGFβ2, but not TGFβ3 (Fig. 2A), whereas those of hepatocyte markers were downregulated by addition of TGFβ1 or TGFβ2 (Fig. 2B). To ascertain that TGFBR2 is also important in the hepatoblast fate decision, HBCs were cultured in medium containing SB-431542, which inhibits TGFβ signaling (Fig. 2C,D). Hepatocyte marker genes were upregulated by inhibition of TGFβ signaling (Fig. 2C), whereas cholangiocyte markers were downregulated (Fig. 2D). To confirm the function of TGFβ1, β2 and β3 in the hepatoblast fate decision, colony assays of the HBCs were performed in the presence or absence of TGFβ1, β2 or β3 (Fig. 2E). The number of CK19 single-positive colonies was significantly increased in TGFβ1- or β2-treated HBCs. By contrast, the number of ALB and CK19 double-positive colonies was reduced in TGFβ1-, β2- or β3-treated HBCs. These data indicated that TGFβ1 and β2 positively regulate the biliary differentiation of HBCs. Taken together, the findings suggested that TGFBR2 might be a key molecule in the regulation of hepato-bilary lineage segregation.

TGFBR2 plays an important role in the cell fate decision of HBCs

To examine whether TGFBR2 plays an important role in the hepatoblast fate decision, *in vitro* gain- and loss-of-function analysis of TGFBR2 was performed in the HBCs. We used siRNA in knockdown experiments (supplementary material Fig. S2) during HBC differentiation on Matrigel. Whereas TGFBR2-suppressing siRNA (si-TGFBR2) transfection upregulated the expression of hepatocyte markers, it downregulated cholangiocyte markers (Fig. 3A). si-TGFBR2 transfection increased the percentage of asialoglycoprotein receptor 1 (ASGR1)-positive hepatocyte-like cells (Fig. 3B). By contrast, it decreased the percentage of aquaporin 1 (AQP1)-positive cholangiocyte-like cells. These results suggest that TGFBR2 knockdown promotes hepatocyte differentiation, whereas it inhibits cholangiocyte differentiation. Next, we used Ad vector to perform efficient transduction into the HBCs (supplementary material Fig. S3) and ascertained *TGFBR2* gene expression in TGFBR2-expressing Ad vector (Ad-TGFBR2)-transduced cells (supplementary material Fig. S4). Ad-TGFBR2 transduction downregulated the expression of hepatocyte markers, whereas it upregulated cholangiocyte markers (Fig. 3C). Ad-TGFBR2 transduction decreased the percentage of ASGR1-positive hepatocyte-like cells but increased the percentage of AQP1-positive cholangiocyte-like cells (Fig. 3D). These results suggest that TGFBR2 overexpression inhibits hepatocyte differentiation, whereas it promotes cholangiocyte differentiation. Taken together, these results suggest that TGFBR2 plays an important role in deciding the differentiation lineage of HBCs.

To investigate whether hepatoblasts would undergo differentiation in a TGFBR2-associated manner *in vivo*, HBCs transfected/transduced with si-control, si-TGFBR2, Ad-LacZ or Ad-
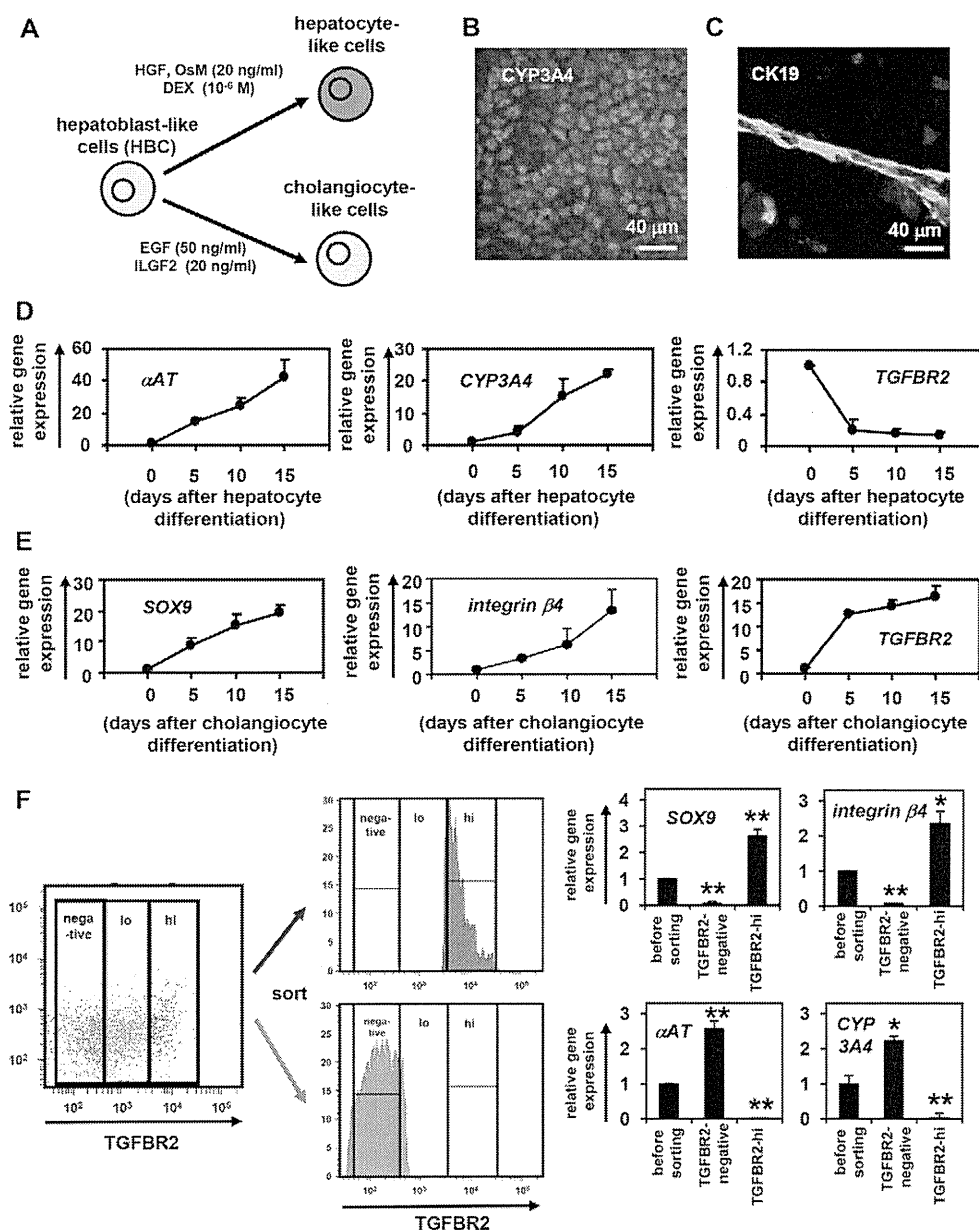
Fig. 1. HBCs can differentiate into both hepatocyte and cholangiocyte lineages. (A) The strategy for hepatocyte and cholangiocyte differentiation from HBCs. (B,C) The HBC-derived hepatocyte-like cells or cholangiocyte-like cells were subjected to immunostaining with anti-CYP3A4 (red, B) or anti-CK19 (green, C) antibodies, respectively. (D,E) Temporal gene expression levels of hepatocyte markers (αAT and CYP3A4) (D) or cholangiocyte markers (SOX9 and integrin β4) (E) during hepatocyte or cholangiocyte differentiation as measured by real-time RT-PCR. The temporal gene expression of TGFBR2 was also examined. The gene expression levels in HBCs were taken as 1.0. (F) HBCs were cultured on Matrigel for 5 days, and then the expression level of TGFBR2 was examined by FACS analysis. TGFBR2-negative, -lo and -hi populations were collected and real-time RT-PCR analysis was performed to measure the expression levels of hepatocyte markers (αAT and CYP3A4) and cholangiocyte markers (SOX9 and integrin β4). *P<0.05, **P<0.01 (compared with 'before sorting'). Error bars indicate s.d. Statistical analysis was performed using the unpaired two-tailed Student's t-test (n=3).

TGFBR2 were transplanted into CCl₄-treated immunodeficient mice (Fig. 3E,F). Although some of the si-control-transfected or Ad-LacZ-transduced HBCs remained as HBCs (HNF4α and CK19 double positive), most of them showed in vitro differentiation toward hepatocyte-like cells (HNF4α single positive) (Fig. 3E, top row). By contrast, Ad-TGFBR2-transduced HBCs were predominantly committed to cholangiocyte-like cells (CK19 single positive) and si-TGFBR2-transfected HBCs were predominantly committed to hepatocyte-like cells (HNF4α single positive) (Fig. 3E, bottom row). Ad-TGFBR2 transduction decreased the percentage of HNF4α-positive hepatocyte-like cells, whereas it increased the percentage of CK19-positive cholangiocyte-like cells (supplementary material Fig. S5). The hepatocyte functionality of the in vivo differentiated HBCs was assessed by measuring secreted human ALB levels in the recipient mice (Fig. 3F). Mice that were transplanted with Ad-TGFBR2-transduced HBCs showed lower human ALB serum levels than those transplanted with Ad-LacZ-transduced HBCs, and the mice that were transplanted with si-TGFBR2-transfected HBCs showed higher human ALB serum

levels than those transplanted with si-control-transfected HBCs. These data suggest that cholangiocyte or hepatocyte differentiation was promoted by TGFBR2 overexpression or knockdown, respectively. Thus, based on these data from in vitro and in vivo experiments, TGFBR2 plays an important role in deciding the differentiation lineage of HBCs.

TGFBR2 promoter activity and expression are negatively regulated by c/EBPα and positively regulated by c/EBPβ

A previous study has shown that TGFBR2 expression is upregulated in Hnf6 knockout mice (Clotman et al., 2005), although we confirmed by ChIP assay that HNF6 does not bind to the TGFBR2 promoter region (data not shown). Because c/EBPα is important in the hepatoblast fate decision (Suzuki et al., 2003), we expected that c/EBPs might directly regulate TGFBR2 expression. The TGFBR2 promoter region was analyzed to examine whether TGFBR2 expression is regulated by c/EBPs. Some c/EBP binding sites (supplementary material Fig. S6) were predicted by rVista 2.0 (http://rvista.dcode.org/) (Fig. 4A). By performing a ChIP assay, one
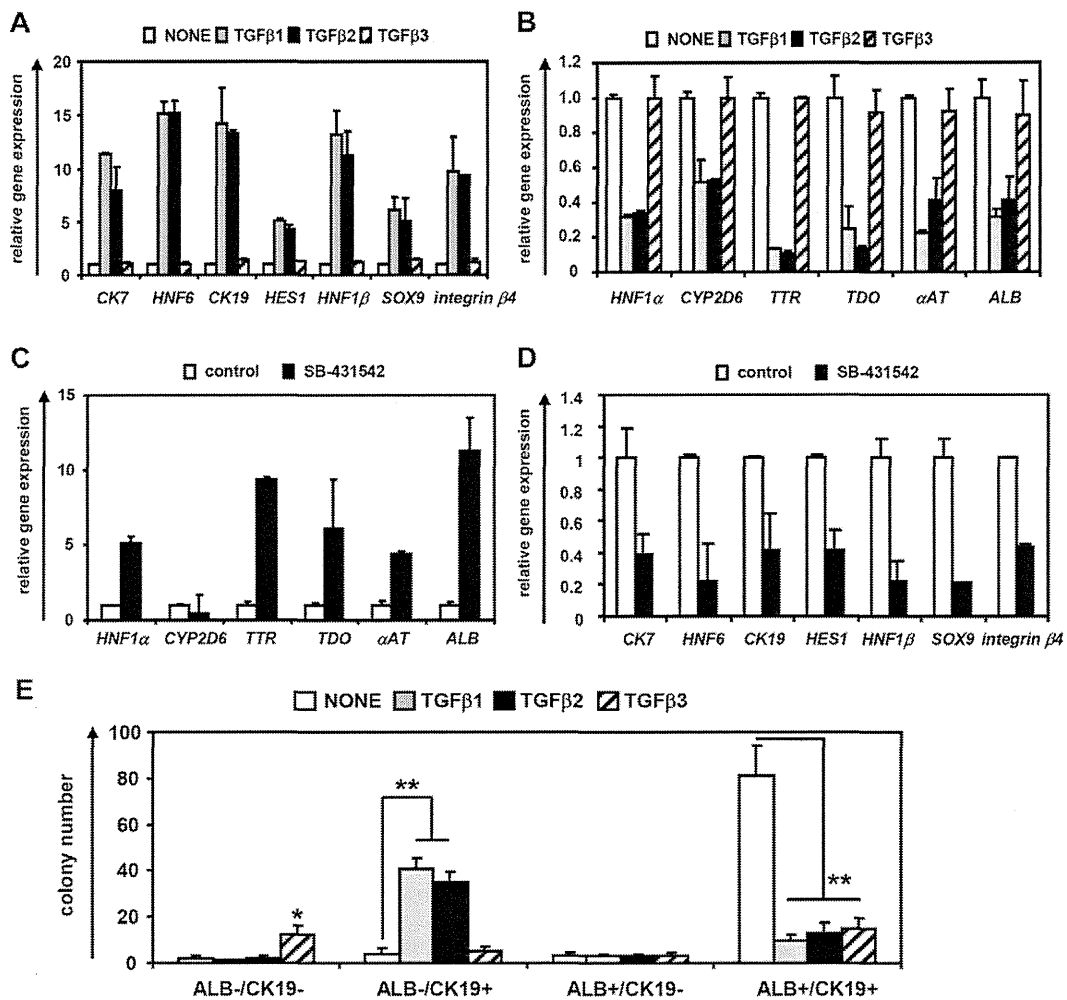
Fig. 2. Hepatocyte and cholangiocyte differentiation from HBCs is regulated by TGFβ signaling. (A,B) HBCs were cultured in differentiation hESF-DIF medium containing 10 ng/ml TGFβ1, TGFβ2 or TGFβ3 for 10 days. The expression levels of cholangiocyte (A) and hepatocyte (B) marker genes were measured by real-time RT-PCR. On the y-axis, the gene expression level of cholangiocyte markers in untreated cells (NONE) was taken as 1.0. (C,D) HBCs were cultured in differentiation hESF-DIF medium containing SB-431542 (10 μM) for 10 days. Control cells were treated with solvent only (0.1% DMSO). Expression levels of hepatocyte (C) and cholangiocyte (D) marker genes were measured by real-time RT-PCR. On the y-axis, the gene expression level of hepatocyte markers in untreated cells (control) was taken as 1.0. (E) HBC colony formation assay in the presence or absence of 10 ng/ml TGFβ1, TGFβ2 or TGFβ3. HBCs were plated at 200 cells/cm² on human LN111-coated dishes. The colonies were separated into four groups based on the expression of ALB and CK19: double-negative, ALB negative and CK19 positive, ALB positive and CK19 negative, and double positive. The numbers represent wells in which the colony was observed in three 96-well plates (total 288 wells). Five days after plating, the cells were fixed with 4% PFA and used for double immunostaining. *P<0.05, **P<0.01 (compared with NONE). Error bars indicate s.d. Statistical analysis was performed using the unpaired two-tailed Student's t-test (n=3).

c/EBP binding site was found in the *TGFBR2* promoter region (Fig. 4B). A reporter assay of the *TGFBR2* promoter region showed that c/EBPβ activates *TGFBR2* promoter activity, whereas c/EBPα inhibits it (Fig. 4C). In addition, *TGFBR2* expression was downregulated by Ad-c/EBPα transduction, whereas *TGFBR2* was upregulated by Ad-c/EBPβ transduction in HepG2 cells (TGFBR2 positive) (Fig. 4D). We ascertained the expression of c/EBPα or c/EBPβ (*CEBPA* or *CEBPB* – Human Gene Nomenclature Committee) in the Ad-c/EBPα- or Ad-c/EBPβ-transduced cells, respectively (supplementary material Fig. S4). These results demonstrated that the promoter activity and expression of *TGFBR2* were directly regulated by both c/EBPα and c/EBPβ.

c/EBPs determine the cell fate decision of HBCs via regulation of TGFBR2 expression

To elucidate the relationship between TGFBR2 and c/EBPs (c/EBPα and c/EBPβ) in the hepatoblast fate decision, we first examined the temporal gene expression patterns of *TGFBR2*, *c/EBPα* and *c/EBPβ* in hepatocyte and cholangiocyte differentiation. During hepatocyte differentiation, *TGFBR2* expression was downregulated, whereas *c/EBPα* was upregulated (supplementary material Fig. S7A, top). During cholangiocyte differentiation, *c/EBPα* was downregulated, whereas *TGFBR2* and *c/EBPβ* were upregulated (supplementary material Fig. S7A, bottom). In addition, the ratio of *c/EBPα* to *c/EBPβ* was significantly increased in hepatocyte differentiation, but significantly reduced in cholangiocyte differentiation (supplementary material Fig. S7B). High-level expression of *c/EBPα* was detected in TGFBR2-negative cells, but not in TGFBR2-hi cells (supplementary material Fig. S7C). By contrast, high-level expression of *c/EBPβ* was detected in TGFBR2-hi cells, but not in TGFBR2-negative cells. These results suggest that TGFBR2 is negatively regulated by c/EBPα and positively regulated by c/EBPβ in the differentiation model from HBCs as well as in the HepG2 cell line (Fig. 4).
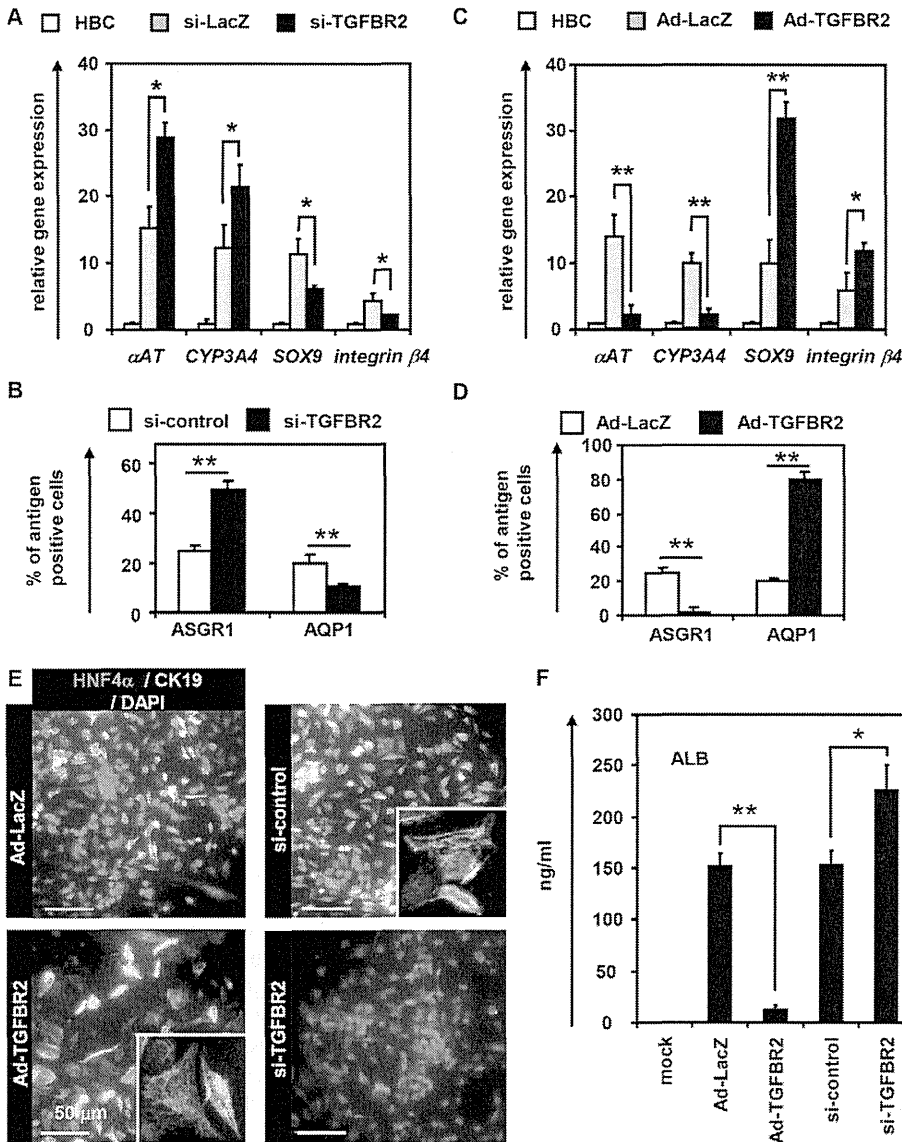
Fig. 3. TGFBR2 regulates bi-directional differentiation of HBCs. (A) HBCs were transfected with 50 nM control siRNA (si-control) or TGFBR2-suppressing siRNA (si-TGFBR2) and cultured in differentiation hESF-DIF medium for 10 days. The expression levels of hepatocyte (αAT and CYP3A4) or cholangiocyte (SOX9 and integrin β4) markers were measured by real-time RT-PCR. On the y-axis, the gene expression level in HBCs was taken as 1.0. (B) On day 10 after siRNA transfection, the efficiency of hepatocyte or cholangiocyte differentiation was measured by estimating the percentage of ASGR1-positive or AQP1-positive cells, respectively, by FACS analysis. (C) HBCs were transduced with 3000 VPs/cell of Ad-LacZ or Ad-TGFBR2 for 1.5 hours and cultured in differentiation hESF-DIF medium for 10 days. Expression levels of hepatocyte or cholangiocyte marker genes were measured by real-time RT-PCR. On the y-axis, gene expression levels in the HBCs was taken as 1.0. (D) On day 10 after Ad vector transduction, the efficiency of hepatocyte or cholangiocyte differentiation was measured by estimating the percentage of ASGR1-positive or AQP1-positive cells, respectively, by FACS analysis. (E,F) The si-control, si-TGFBR2, Ad-LacZ- or Ad-TGFBR2-transfected/transduced HBCs (1.0×10^6 cells) were transplanted into CCl4-treated (2 mg/kg) Rag2/Il2rg double-knockout mice by intrasplenic injection. (E) Expression of human HNF4α (red) and CK19 (green) was examined by double immunohistochemistry 2 weeks after transplantation. Nuclei were counterstained with DAPI (blue). (F) Levels of human ALB in recipient mouse serum were measured 2 weeks after transplantation. *P<0.05, **P<0.01 (compared with Ad-LacZ-transduced or si-control-transfected cells). Error bars indicate s.d. Statistical analysis was performed using the unpaired two-tailed Student's t-test (n=3).

ChIP experiments showed that c/EBPα or c/EBPβ is recruited to the *TGFBR2* promoter region containing the c/EBP binding site in hepatocyte-like cells or cholangiocyte-like cells, respectively (Fig. 5A), suggesting that c/EBPα and c/EBPβ oppositely regulate *TGFBR2* promoter activity in the differentiation from HBCs. We confirmed that c/EBPα or c/EBPβ was mainly recruited to the *TGFBR2* promoter region containing the c/EBP binding site in TGFBR-negative or TGFBR2-positive cells, respectively (supplementary material Fig. S7D). Taken together, we concluded that c/EBPα and c/EBPβ are able to regulate the cell fate decision of HBCs via regulation of TGFBR2 expression. During differentiation from HBCs, *TGFBR2* expression was negatively regulated by c/EBPα and positively regulated by c/EBPβ (Fig. 5B). To examine whether c/EBPα or c/EBPβ could regulate the differentiation from HBCs, *in vitro* gain- and loss-of-function analyses were performed. si-c/EBPα transfection downregulated hepatocyte marker gene expression, whereas it upregulated cholangiocyte marker genes (Fig. 5C). By contrast, si-c/EBPβ transfection upregulated hepatocyte marker and downregulated cholangiocyte marker gene expression (Fig. 5C). In accordance, Ad-c/EBPα transduction upregulated hepatocyte marker genes and downregulated cholangiocyte markers (Fig. 5D), whereas Ad-

c/EBPβ transduction downregulated hepatocyte markers and upregulated cholangiocyte marker genes. Promotion of hepatocyte differentiation by Ad-c/EBPα transduction was inhibited by Ad-TGFBR2 transduction, whereas inhibition of cholangiocyte differentiation by Ad-c/EBPα transduction was rescued by Ad-TGFBR2 transduction (Fig. 5E). In addition, promotion of hepatocyte differentiation by si-c/EBPβ transfection was inhibited by Ad-TGFBR2 transduction, whereas inhibition of cholangiocyte differentiation by si-c/EBPβ transfection was rescued by Ad-TGFBR2 transduction (Fig. 5F). We further confirmed that inhibition of hepatocyte differentiation by si-c/EBPα-transfection was rescued by si-TGFBR2 transfection (supplementary material Fig. S8). Taken together, these results led us to conclude that c/EBPα and c/EBPβ could determine the cell fate of HBCs by negatively and positively regulating TGFBR2 expression, respectively (supplementary material Fig. S9).

c/EBPs organize the differentiation of fetal mouse hepatoblasts through regulation of TGFBR2 expression

We have demonstrated that c/EBPs may determine the HBC fate decision via regulation of the expression level of TGFBR2. To examine whether our findings could be replicated in native liver